materials

MDPI

Review

Properties and Applications of Geopolymer Composites: A Review Study of Mechanical and Microstructural Properties

Ahmed Saeed [1,*], Hadee Mohammed Najm [2,*], Amer Hassan [2], Mohanad Muayad Sabri Sabri [3], Shaker Qaidi [4,5], Nuha S. Mashaan [6] and Khalid Ansari [7]

1 Department of Civil Engineering, Southeast University, Nanjing 211189, China
2 Department of Civil Engineering, Zakir Husain Engineering College, Aligarh Muslim University, Aligarh 202002, India
3 Peter the Great St. Petersburg Polytechnic University, 195251 St. Petersburg, Russia
4 Department of Civil Engineering, College of Engineering, University of Duhok, Duhok 42001, Iraq
5 Department of Civil Engineering, College of Engineering, Nawroz University, Duhok 42001, Iraq
6 Faculty of Science and Engineering, School of Civil and Mechanical Engineering, Curtin University, Bentley, WA 6102, Australia
7 Department of Civil Engineering, Yashwantrao Chavan College of Engineering, Nagpur 441110, India
* Correspondence: alanessy2015@gmail.com (A.S.); gk4071@myamu.ac.in (H.M.N.)

Abstract: Portland cement (PC) is considered the most energy-intensive building material and contributes to around 10% of global warming. It exacerbates global warming and climate change, which have a harmful environmental impact. Efforts are being made to produce sustainable and green concrete as an alternative to PC concrete. As a result, developing a more sustainable strategy and eco-friendly materials to replace ordinary concrete has become critical. Many studies on geopolymer concrete, which has equal or even superior durability and strength compared to traditional concrete, have been conducted for this purpose by many researchers. Geopolymer concrete (GPC) has been developed as a possible new construction material for replacing conventional concrete, offering a clean technological choice for long-term growth. Over the last few decades, geopolymer concrete has been investigated as a feasible green construction material that can reduce CO_2 emissions because it uses industrial wastes as raw materials. GPC has proven effective for structural applications due to its workability and analogical strength compared to standard cement concrete. This review article discusses the engineering properties and microstructure of GPC and shows its merits in construction applications with some guidelines and suggestions recommended for both the academic community and the industrial sector. This literature review also demonstrates that the mechanical properties of GPC are comparable and even sometimes better than those of PC concrete. Moreover, the microstructure of GPC is significantly different from that of PC concrete microstructure and can be affected by many factors.

Keywords: geopolymer composites; clean technology; flexural strength; compressive strength

Citation: Saeed, A.; Najm, H.M.; Hassan, A.; Sabri, M.M.S.; Qaidi, S.; Mashaan, N.S.; Ansari, K. Properties and Applications of Geopolymer Composites: A Review Study of Mechanical and Microstructural Properties. *Materials* **2022**, *15*, 8250. https://doi.org/10.3390/ma15228250

Academic Editors: Arslan Akbar and Shouke Yan

Received: 13 August 2022
Accepted: 17 November 2022
Published: 21 November 2022

1. Introduction

Concrete is a widely utilised material in the building industry worldwide [1]; because of its low cost, durability, strength, and flexibility to be produced in any shape or size, it is considered the most extensively material used in building [2]. PC is one of the most energy-intensive building materials used in reinforced concrete applications, with current output estimated to be 2.60 billion tonnes (BT) per year worldwide and increasing by 5% annually. PC is made using the "two grinding and one calcining" technology, which uses limestone, clay, and other raw materials as inputs, with a calcination temperature of 1450 °C. Approximately one billion tonnes (BT) of limestone, 180 MT of clay, 50 MT of iron powder, 100 MT of coal, and 60 B KWh of energy are used annually by the cement industry in China [3]. A lot of carbon dioxide is released into the air during cement manufacturing

(one tonne of cement production emits approximately one ton of CO_2). Extremely high carbon dioxide levels are released into the air during the cement manufacturing process (roughly one tonne of cement production releases one tonne of CO_2). This causes it to account for about 7% of all manufactured CO_2 emissions. Table 1 [4] summarises the amount of carbon dioxide released during the construction of various concrete elements.

Table 1. CO_2 emissions from different concrete volumes [4].

Strength (MPa)	Structural Member	Amount (m^3)	Emission Factor ($tCO_2{}^{-e}/m^3$)	Emissions ($tCO_2{}^{-e}$)
15	Blinding	589	0.20	119
32	Footings	489	0.24	119
32	Slabs	1984	0.27	533
40	In situ column and wall	253	0.27	63
40	Precast walls	1067	0.33	351–1185

Additionally, Figure 1 presents the global trends in growing cement production. Limestone calcining and using a rotary kiln powered by fossil fuels to provide high heat contribute to substantial CO_2 emissions; this is a significant concern when utilising the PC. One of the most promising options is using geopolymers as a partial or complete substitute for cement [5,6].

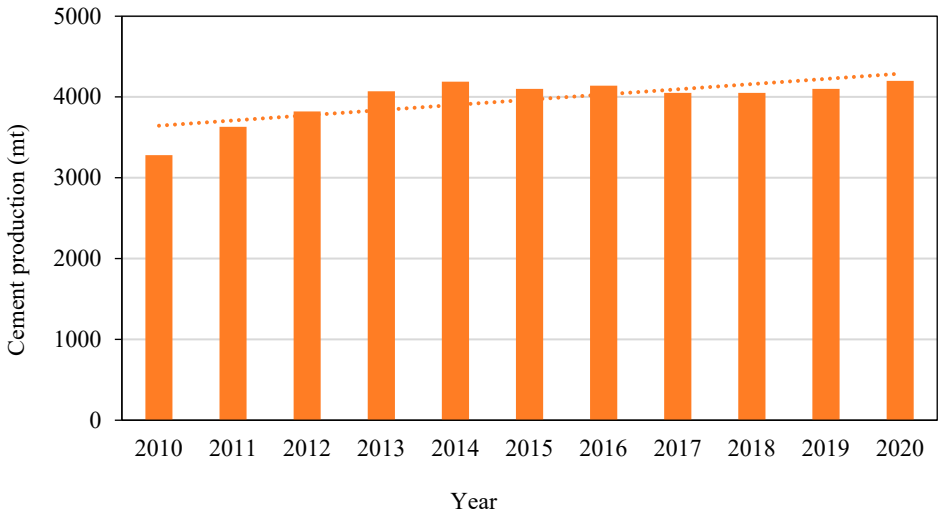

Figure 1. Worldwide cement production in Metric Tonnes, 2010–2020 [7].

In 1979, Davidovits introduced the term geopolymer to refer to a group of mineral binders similar to zeolites within amorphous microstructure and chemical composition [8]. This material was previously used in the Roman Empire (Figure 2). An aluminosilicate precursor (Figure 3), made up of amorphous silica and alumina, and an activator (a dissolving agent) make up the geopolymers. The term "geopolymerisation" describes the transformation of zeolitic-like materials into a 3D aluminosilicate gel [9–12]. Generated binder performance is optimised through an alkaline polycondensation process involving silicate and aluminate [13]. It is a common practise to use caustic alkalis of the MOH type or silicates of the $R_2O(n)SiO_2$ type in the synthesis of geopolymers. Sodium hydroxide (NaOH), sodium carbonate ($NaCO_3$), potassium hydroxide (KOH), or sodium sulphate (Na_2SO_4) are common activators that contain the alkali metal (M) indicated by MOH [14]. In addition to the conventional activators, silica fume and rice husk ash have also been used as activator components in the synthesis of geopolymers [15].

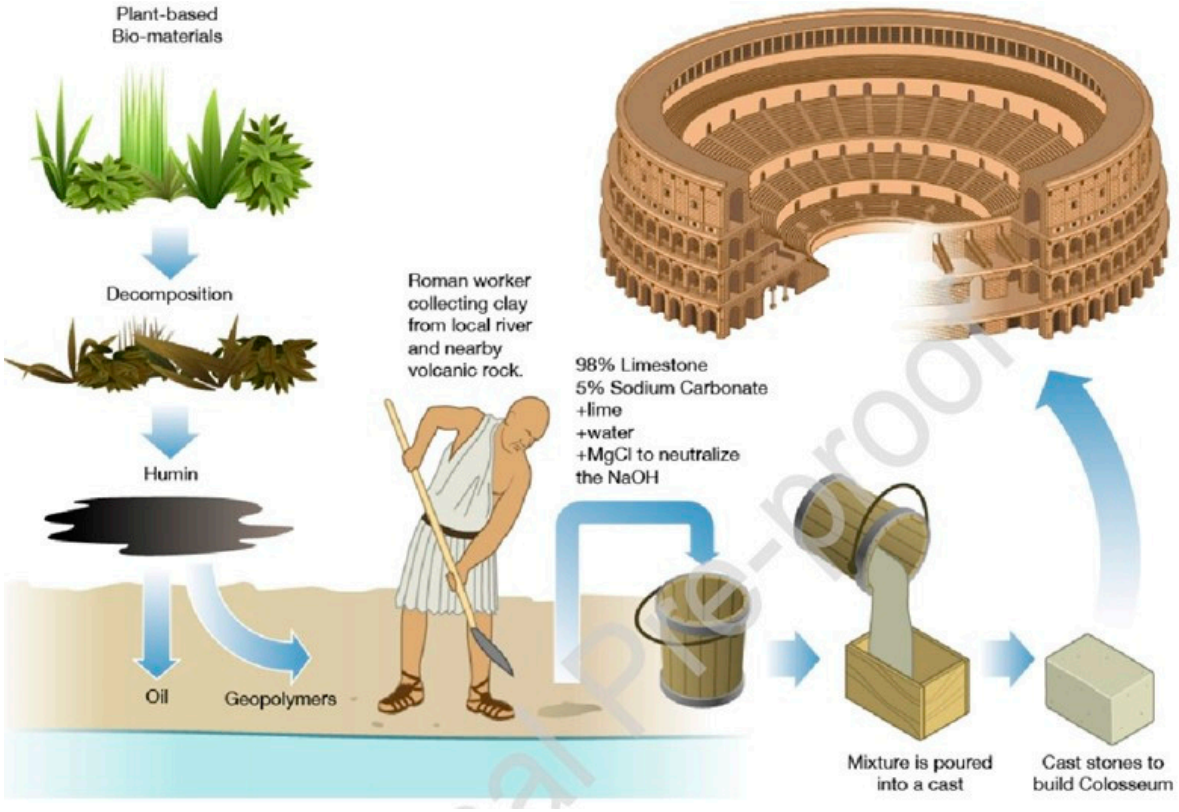

Figure 2. Manufacturing Process of GPCs in the Roman Kingdom [16].

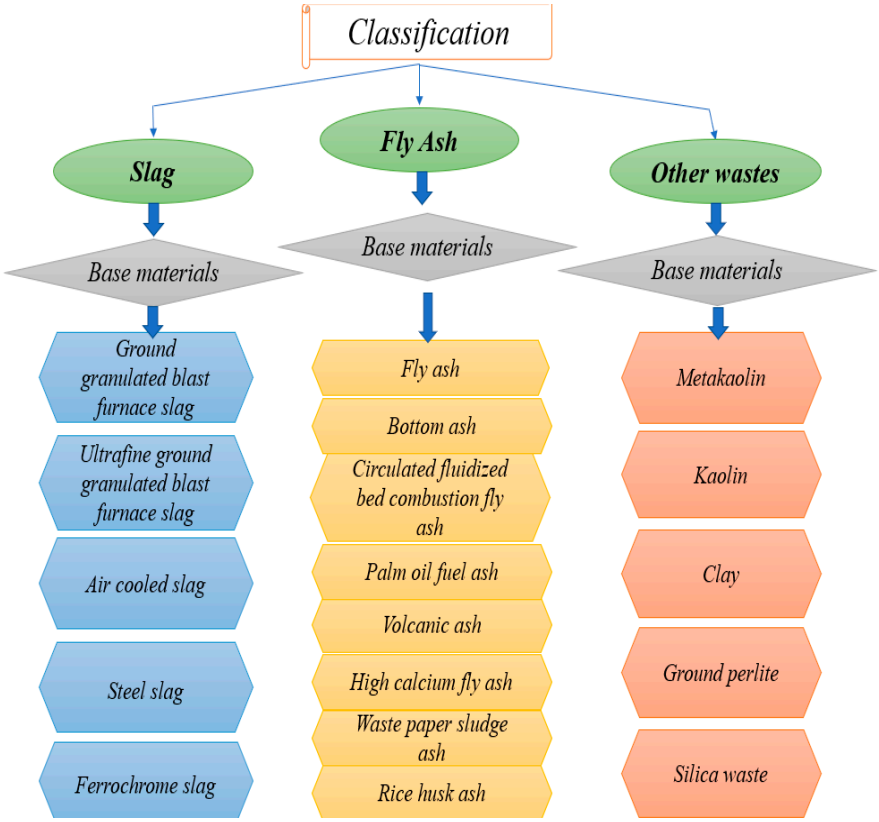

Figure 3. Raw materials used in geopolymer production.

The environmental benefits of geopolymer concrete have led many to call it the "next generation" of concrete. It provides a novel approach to reducing CO_2 emissions in the construction industry by abolishing PC as a binder in concrete production [1,17,18]. Using geopolymer concrete not only has positive effects on the environment and human health but also provides a method for safely disposing of potentially hazardous materials [19]. In addition, research shows that the production of geopolymer concrete can reduce CO_2 emissions by about 22–72% compared to that of PC concrete at a similar cost [20]. In addition, tests [21–24] have confirmed that geopolymer concrete has exceptional mechanical properties. Geopolymer concrete (shown in Figure 4) is a sustainable building material depicted in a simplified diagram.

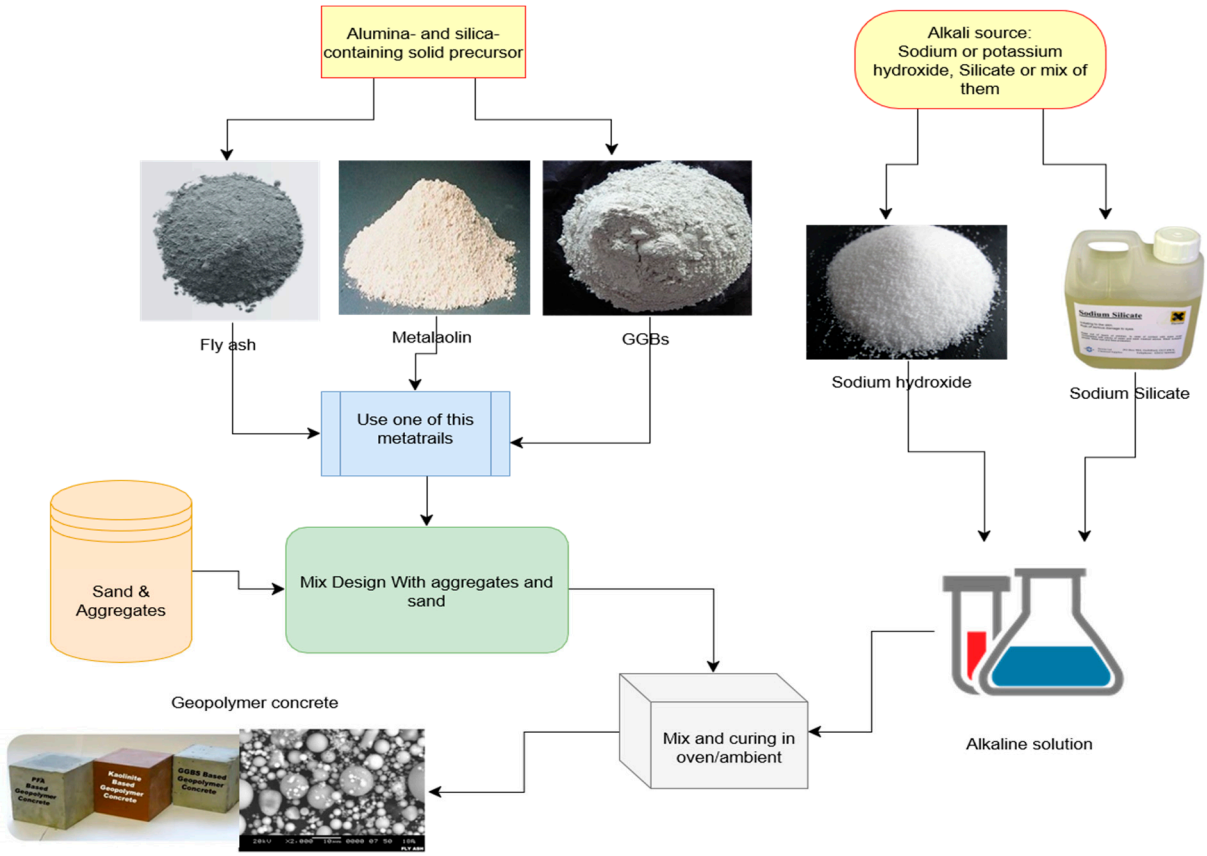

Figure 4. Geopolymer concrete production [25].

It was observed in the literature that there are many existing review studies to analysing the behaviour of geopolymer concrete [1–15,17,26–34]. However, previous review publications on geopolymer composite mortar/concrete highlighted mechanical or microstructural properties in the fresh and hardened states. However, they did not provide comprehensive information on this issue in a single paper. In addition, new studies that are relevant to the topic but were not discussed in earlier reviews were published. Therefore, this study provides a comprehensive overview of the most up-to-date studies on geopolymer concrete's mechanical and microstructural performance. It includes a review, analysis, and discussion of the literature on geopolymer concrete in its fresh and hardened states to aid in the education of researchers and the building industry.

Study Significance

The published literature papers were evaluated regarding the production of GPC and its mechanical behaviour. This paper discusses the mixed design, mechanical characteristics, and durability of GPC. Using the GPC as an alternative construction material is essential for environmental purposes. Before it can be used in construction, much research needs to be conducted on how structures behave with huge structural elements.

Therefore, this review article aims to provide inclusive information on GPC production, its economic benefits, durability, and environmental influences; the basic process for GPC production; and the factors affecting its mechanical properties.

2. Geopolymer Mortar (GPM)

Classic cement mortar is often utilised as a standard binding and repairing material in various engineering structures. Many scholars have addressed GPM's viability and potential applications as a suitable replacement for regular cement mortar [35]. Sathonsaowaphak was the first to investigate geopolymer mortar and studied the properties of bottom ash fineness, ash/liquid alkali ratio, NaOH/Na_2SiO_3 ratio, NaOH dosage, water to ash ratio, and superplasticiser on the behaviour in terms of workability and compressive strength of GPM [36]. Geopolymer mortar has a mechanical strength of 24–58 MPa, and adding NaOH solution improves the workability performance of GPM without reducing strength. According to the results of Detphan and Chindaprasirt [24], who prepared GPC using rice husk ash and fly ash and activated by NaOH and $NaSiO_3$ solution as a liquid for the mix, they found that the maximum strength of GPM is acquired by employing a Na_2SiO_3-to-NaOH mass ratio of four. Moreover, more discussion about geopolymer mortar properties is reported in the following sections.

2.1. Fresh Geopolymer Mortar Properties

2.1.1. Fresh Geopolymer Mortar Workability

The workability of fresh GPM is crucial in determining the hardened GPM quality. The concentration ratio of NaOH determines the geopolymer mortar's workability and the Na_2SiO_3 to NaOH. The flowability of modern mortars is typically controlled with the addition of water, which does not compromise the mortar's strength [37]. Flow, which a flow test may evaluate, is frequently used to determine whether mortar is workable. The term "flow" is widely used to describe how well new mortars work, and it is given as a percentage of the starting base diameter as per the ASTM C1437 standard [38]. Some testing instruments include a flow mould, measuring tape, tamper, flow table, and trowel. The flow test determines a material's consistency, filling ability, and workability. Sathonsaowaphak [36] studied the effect of bottom ash (BA) fineness on mortar workability and suggested that ground bottom ash might be employed as a raw material for the production of geopolymer. When the fineness of BA was increased, the workability of the mortar was improved. (Figure 5), as well as the impact of various liquid ratios of alkaline/ash. The workability of the mixes improved as the liquid alkaline/ash ratio was raised, as seen in Figure 6.

Bhowmick and Ghosh [39] determine the impact of fly ash/sand ratios and the influence of SiO_2/Na_2O ratio inactivators on GPM workability. They found that the flow value percentage increases with the fly ash/sand ratio, and the fresh geopolymer mortar's flowability increases as the SiO_2/Na_2O ratio in the activator increases, as shown in Figures 7 and 8.

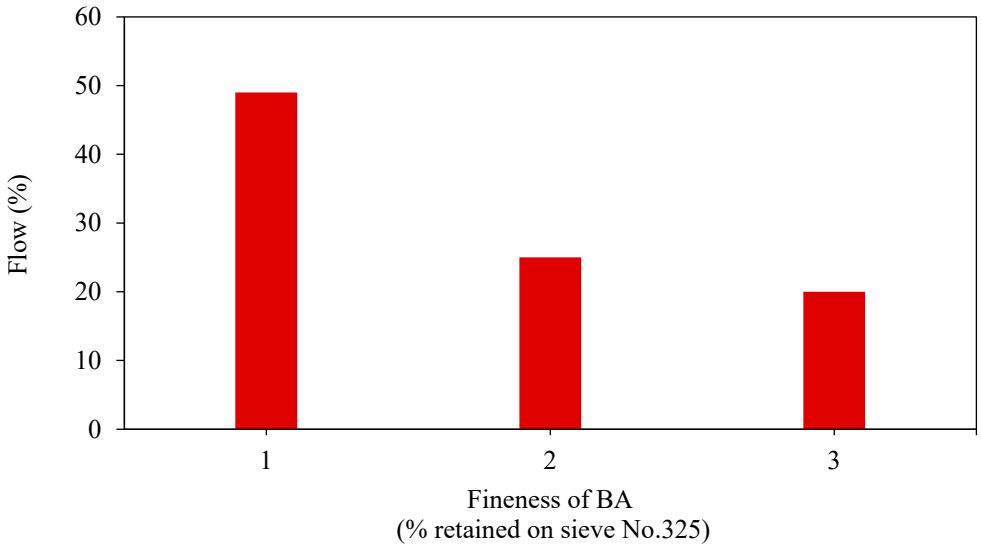

Figure 5. The flow of mortar with various BA fineness [36].

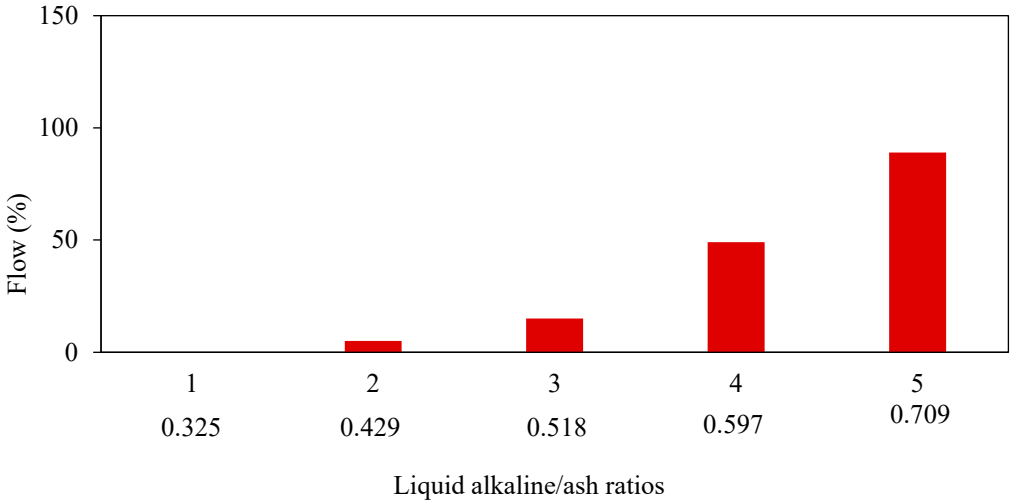

Figure 6. The flow of mortar with various liquid alkaline-to-ash ratios [36].

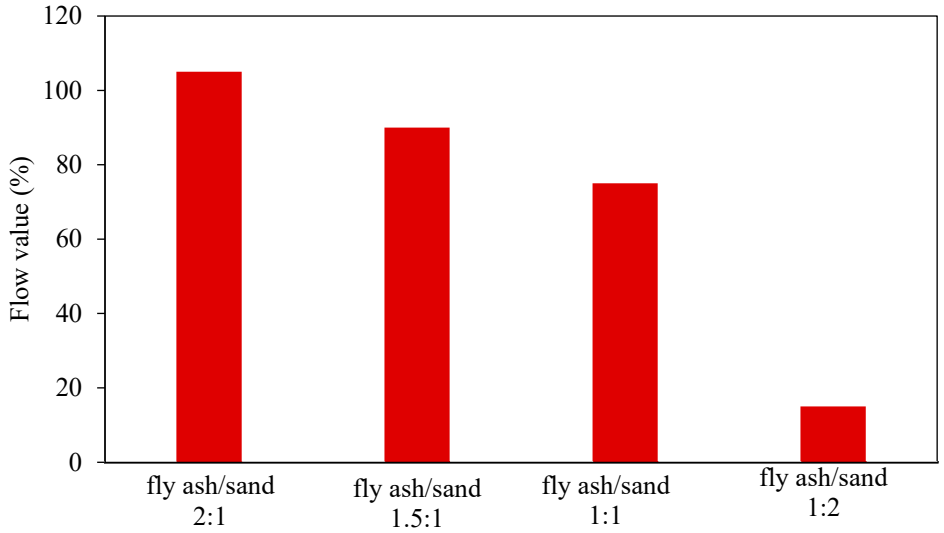

Figure 7. Flow value vs. fly ash/sand ratio [39].

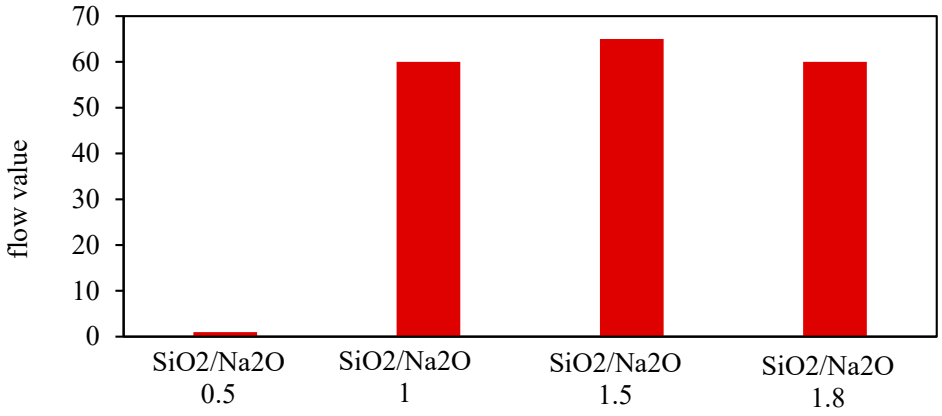

Figure 8. Flow value vs. SiO_2/Na_2O ratio in activator [39].

2.1.2. Fresh Geopolymer Mortar Setting Time

Fresh mortar setting time is critical for transporting, casting, and compacting the mortar within the time restriction. The Vicat needle device can be utilised to test the setting times per the BS EN 480-2 and ASTM C 807-13 standards [40,41]. The first and final setting times are calculated using the needle's depth as a reference point, which ranges between 2.5 and 4 mm [41,42]. In order to determine the influence of time after mixing on dielectric properties before heat curing, cast specimens were kept in a laboratory at 28 to 29 °C while being protected from moisture loss by a vinyl sheet geopolymer. The dielectric characteristics of GPM were then measured after being mixed for 24 h [42]. Jumrat et al. [42] investigated the setting time of the specimen's mixture with the addition of water to obtain the standard flow. The results demonstrate that the weight proportions of NS/NH and FA/AS do not affect the initial and final setup periods. The setting time reduces as NS/NH and FA/AS weight ratios increase, as shown in Figure 9 [24]. By increasing the molarity of NaOH, the initial and final setting times of GPM can be greatly decreased [43].

The setting time reduction in GPM has been attributed to the increased use of PCs. As seen in Figure 10, increased NaOH concentrations caused geopolymer mortars to take longer to set [44].

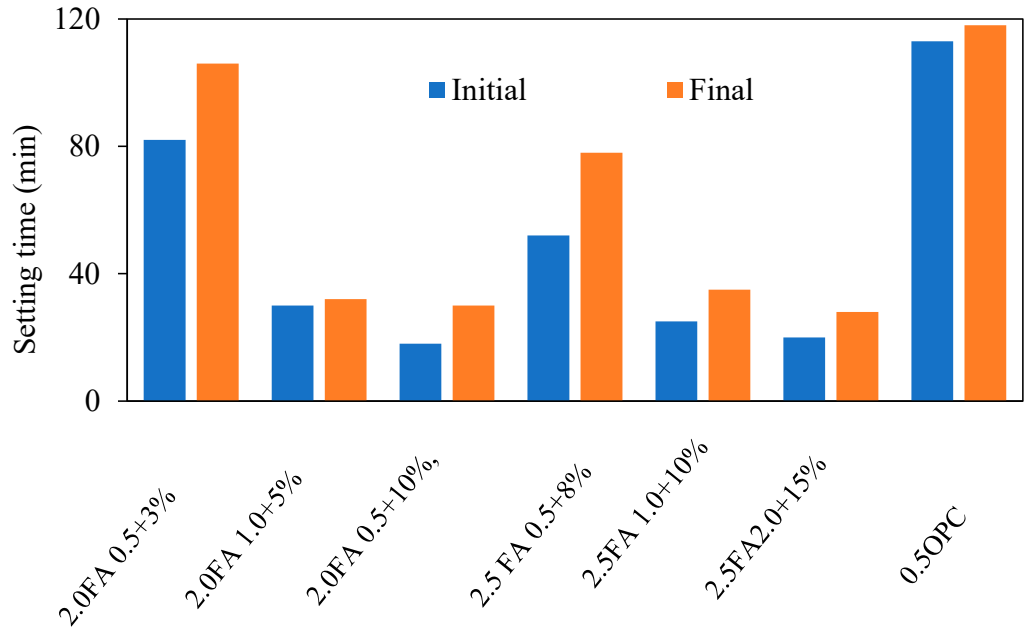

Figure 9. GPM setting times at different mixture proportions [42].

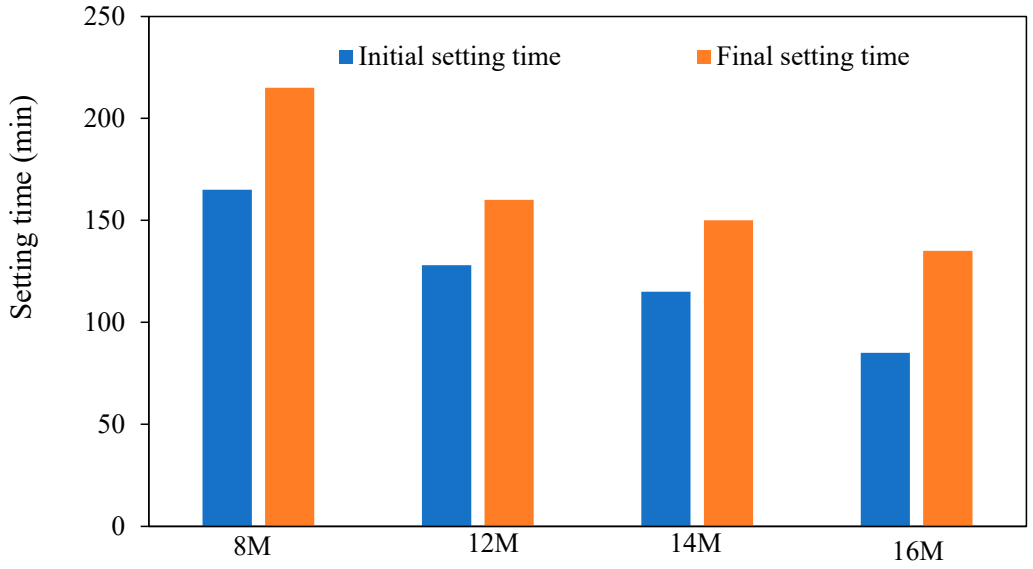

Figure 10. Effect of NaOH molarity on GPM setting times [43].

2.2. Geopolymer Mortar Mechanical Properties

2.2.1. Geopolymer Mortar Compressive Strength

Numerous types of source materials are employed as base materials for producing geopolymers. The raw materials used and the proportioning factors impact the strength of GPM. A. Erfanimanesh et al. [45] tried to compare the compressive strength of GPM at the ages of 7 and 28 days, using two different mixed materials (PC mortar, slag, and zeolite). The findings revealed that the compressive strength of GPM increased by up to 48% in the first 7 days compared to the cement mortar after 28 days.

Yusuf et al. [46] studied the effect of blending silica-rich (MK) and palm oil fuel ash (POFA) on the strength of GPM. They indicated that the Weibull distribution is suitable for analysing the blended GPM. Low calcium FA, GGBFS, and POFA can be combined to manufacture GPM under the standard condition that their percentage should be suitable. Ismail et al. [47] investigated the early strength characteristics of a GPM made from palm oil fuel and ash metakaolin with various degrees of NaOH and Na_2SiO_3 medium replacement. Ismail et al. [47] studied the compressive strengths of GPM with sisal fibre (SF), coconut fibre (CF), and glass fibre (GF).

Phoo et al. [44], who studied the compressive strength of GPM with different NaOH dosages (6, 10, and 14 mol/dm^3), found that high calcium FA GPM comprised of PC type I showed increasing PC replacement levels and NaOH concentrations as well as increasing mortar compressive strengths.

A. De Rossi [48] discovered that the strength of geopolymer mortars was affected by the use of construction and demolition waste (CDW) fine aggregates. GPM was formed by combining biomass FA waste and MK as a binder, sodium hydroxide as an activator, alkali sodium silicate solution, and CDW as fine aggregates. Except for the mortar created with particles of 1.0–2.0 mm, when the maximum strength was acquired with sand, CDW was used as aggregate. For CDW–geopolymer mortars, the values were 21 MPa (1.0–2.0 mm), 34 MPa (0.5–1.0 mm), and 40 MPa (0.5–2.0 mm). The mixed fraction had the highest strength values due to the maximum packing density. Table 2 illustrates the effect of various additives on the behaviour of geopolymer mortar.

Table 2. Effect of different additives on geopolymer concrete compressive strength.

Ref.	Additives	Remarks
Erfanimanesh et al. [45]	PC mortar, slag, and zeolite	The compressive strength of GPM increased by up to 48% in the first seven days compared to the cement mortar after 28 days.
Tanakorn Phoo [44]	NaOH dosages	A high NaOH dosage increases mortar compressive strengths.
Mohammad Ismail et al. [47]	palm oil fuel and ash metakaolin	The high volume of palm oil fuel and ash metakaolin replacement has been found to reduce compressive strength at an early curing age.
Yusuf et al. [46]	blending silica-rich MK and palm oil fuel ash	The Weibull distribution is suitable for analysing the blended GPM.
Ismail et al. [47]	sisal fibre (SF), coconut fibre (CF), and glass fibre (GF)	The compressive strengths of GPM reinforced with SF, CF and GF both dropped a lot more than those reinforced with SF.
De Rossi [48]	construction and demolition waste (CDW)	The mixed fraction had the highest strength values due to the maximum packing density.

2.2.2. Geopolymer Mortar Flexural Strength

In cement mortars, compressive and flexural strength are tightly linked. However, due to the incredible fragility of the geopolymer and its firm adherence to the aggregate particles, geopolymer mortars have high flexural strength but poor compressive strength [49]. With the addition of sand concentration to 77%, the flexural strength of GPM improves and reaches its maximal value, which slowly decreases because there is an insufficient binder to hold the grains together [20]. Thus, these findings indicate the formation of coarse pores and increased porosity. The alkali activator solution type and curing temperature impact GPM's flexural strength considerably [50]. According to the results of Huseien et al. [50], the GPM with a curing temperature of 28 °C has higher flexural strength than mortars with curing temperatures of 60 °C and 90 °C. Additionally, the activator solution of sodium aluminosilicate hydrate has lower flexural strength than the sodium hydroxide solution [51]. Li et al. [52] studied the influence of curing conditions on the strength of Class-C FA geopolymer at W/F0.35, where he concluded "For Class-C FA GPM with a water/ash ratio of 0.35 (CF35-C), the findings showed that before the age of 7 d, the non-standard curing shows much higher flexural strength than the standard curing. After steam curing for 24 h and 6 h, flexural strength increased sharply at the age of 1 d; then, strength developed slowly". Atis et al. [53] studied the flexural strength of GPM with various sodium concentrations and cured it for 24, 48, and 72 h at temperatures ranging from 45 °C to 116 °C. Atis et al. [53] showed the GPM containing 13% sodium after 24 h of heat curing at 116 °C had the maximum flexural strength, while the GPM incorporating 4.0% sodium after 24 h of heat curing at 106°C had the lowest flexural strength. Al-Majidi et al. [54] investigated the effect of Ground granulated blast-furnace slag (GGBFS) content on the ultimate flexural strength of GPM specimens cured at ambient temperature and variations in flexural strength with increasing GGBFS volume at curing ages of 7, 14, and 28 days; the results showed that at all ages, increasing the GGBFS content increased the ultimate flexural strength of GPM significantly. At 7 days, the flexural strength was improved by increasing the GGBFS content from 10 to 20, 30, and 40%, respectively. Flexural strength increased with longer curing durations, with flexural strength values for 10S, 20S, 30S, and 40S combinations rising at 14 and 28 days, respectively, compared to flexural strength values at 7 d. This is seen in Figure 11.

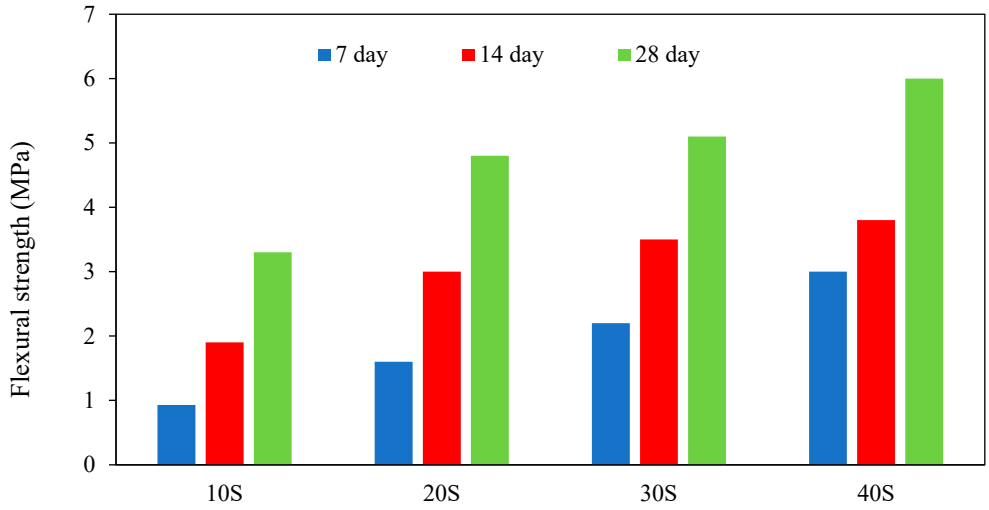

Figure 11. Influence of GGBFS volume on the ultimate flexural strength of GPM [54].

According to Erfanimanesh et al. [45], flexural strength comparison between GPM and PC mortar (Na_2CO_3 concentration was about 10% by weight of powder mixes (zeolite and slag), and 100% Fine Aggregate). GPM's flexural strength was tested using two distinct mix designs that used slag and zeolite as base ingredients. As shown in Figure 12, the geopolymer and the PC mortars had nearly comparable flexural strengths.

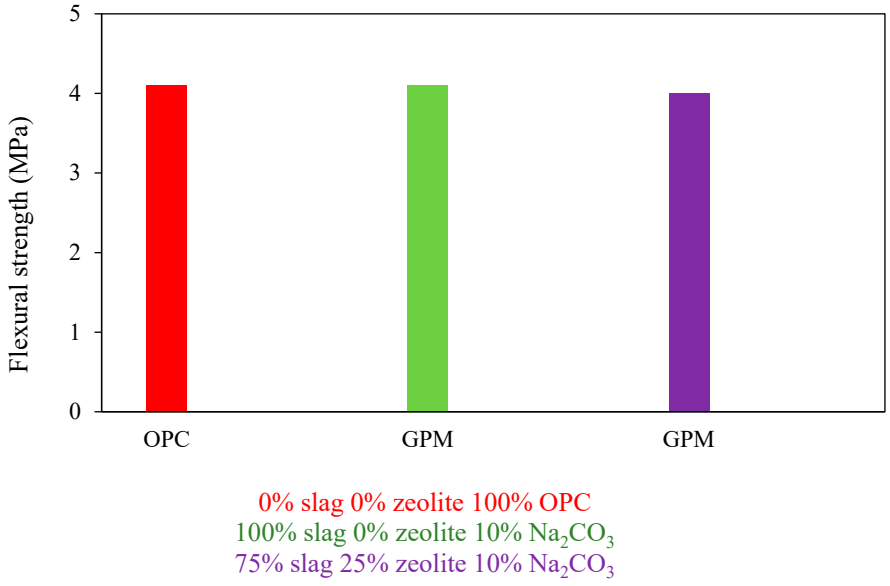

Figure 12. Flexural strength comparison between GPM and PCM.

Wongsa et al. [55] examined the properties of GPM comprising natural fibres and high levels of calcium fly ash. The primary materials in this investigation included coir or coconut fibre (CF), glass fibre (GF), and sisal fibre (SF). SF and CF were acquired from a plant farm in the Thai provinces of Prachuap Khiri Khan and Chon Buri, respectively. According to the results, utilising fibres enhanced GPM's flexural strength. In addition, the flexural strength of GPM tended to increase as the fibre content increased. Even though flexural strengths increased with fibre content, the mixtures with more than 1% volume fraction had poor workability and were challenging to compact and cast. The flexural strength of GPM reinforced with natural fibre (CF and SF) varied from 5.3 to 6.6 MPa compared to CGM (3.2 MPa) and GPM reinforced with synthetic fibre (GF) (3.1–3.7 MPa), as shown in Figure 13.

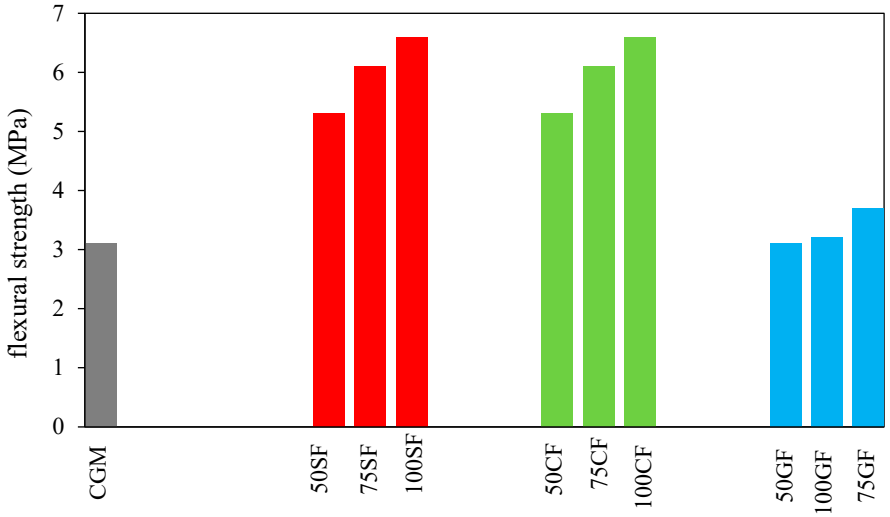

Figure 13. Flexural strength of GPM [55].

3. Geopolymer Concrete (GPC)

GPC is a cost-effective alternative that can be applied in place of standard cement. Thus, using GPC instead of PC cuts CO_2 emissions dramatically [25]. FA, MK, and GGBFS are examples of GPC sources, including Al and Si as rich materials [56]. GPC consists of three components: GGBFS, or MK, a source of aluminosilicates, such as FA; coarse and fine aggregate; and an activating solution consisting of sodium hydroxide and sodium silicate [20]. GGBS, FA, and MK, among other supplemental cementitious materials, are utilised as binders rather than cement. Using GGBS in combination with PC, FA, and palm oil fuel ash results in a high-strength GPC [16]. FA is the substance most frequently employed in the creation of GPCs as a single source of material [24]. Geopolymer concrete emits 20% less CO_2 than PC when (5–15%) Portland cement is substituted. This is because geopolymer concrete may attain an early compressive strength of 66 without needing external heat [20]. In order to create geopolymer paste, an inorganic polymeric binder, the source material must be combined with the activator, a solution of NaOH and Na_2SiO_3. Despite minimising the cost of GPC, no research on the availability and cost of GPC raw materials has been conducted globally. A global review of raw materials availability has been conducted, focusing on China and the U.S. The demand and cost of each raw material, including FA, SC, MK, NaOH, Na_2SiO_3, and silica fume, were analysed for China, the United States, and other major markets for which data are available. This study is essential to see if GPC can be a viable commercial alternative to PC concrete. Raw material supply is a pivotal impediment to widespread GPC adoption [23], so while the cost of each material is listed and briefly addressed, a more in-depth cost study was not conducted.

3.1. Fresh Properties of Geopolymer Concrete

3.1.1. Geopolymer Concrete Workability

Umniati et al. [29] highlighted that the workable flow of the GPC increases as the fly ash/sand ratio increases, and the sodium silicate solution's cohesion and slump ability improve when the SiO_2/Na_2O ratio rises [14]. Saranya et al. [23] also used the IS-1199:1959 slump cone test to find out how the different workable samples of GPC were. Due to its dense flow character, the slump value of GPC specimens was 72% higher than that of cement concrete. Steel fibres limit workability because they block the flow of concrete. Mehta et al. [30] studied the workability of GPP, and GPC was investigated at different molarities of NaOH and varied SiO_2/Al_2O_3 ratios by mass. Because the particles on the alkaline activator mixture grow as the dosage of NaOH increases, it is also noted that the dosage of NaOH considerably impacts the workability of GPC.

Hassan et al. [31] evaluated the workability of FA-based GPC using the slump cone test. Coarse and fine aggregate, alkaline liquid, FA, and water are used in GPC. Sodium silicate and sodium hydroxide are combined to make the alkaline liquid. As shown in Figure 14, the findings of the experiments showed that adding GGBS makes GPC less workable.

Sarker et al. [16] examined the feasibility of fly ash-based GPC for curing in ambient conditions. The experimental results showed that the slump and flow parameters are reduced in FA-based GPC when the slag blend increases. The behaviour becomes more visible as the percentage of the blend increases. As shown in Figure 15, S00, S10, S20, and S30 represent combinations with slag contents of 0%, 10%, 20%, and 30%, respectively.

The steel and iron industries produce ground granulated blast furnace slag (GGBS). According to Patilet et al. [57], using GGBS in concrete increases the material's workability, among other benefits. Geopolymer concrete made from ground-granulated blast furnace slag was developed by Rajarajeswari et al. [58].

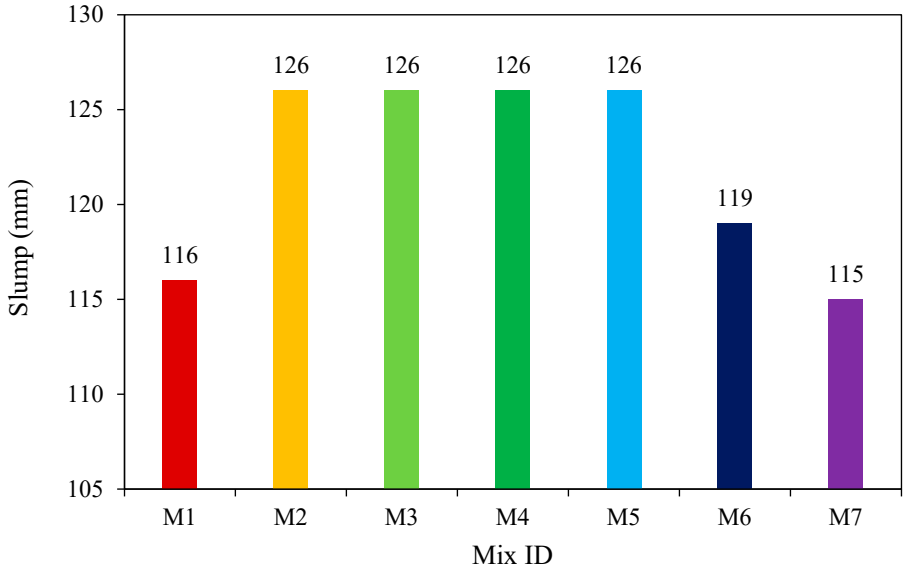

Figure 14. Variation in slump for different mixes (mm) [31].

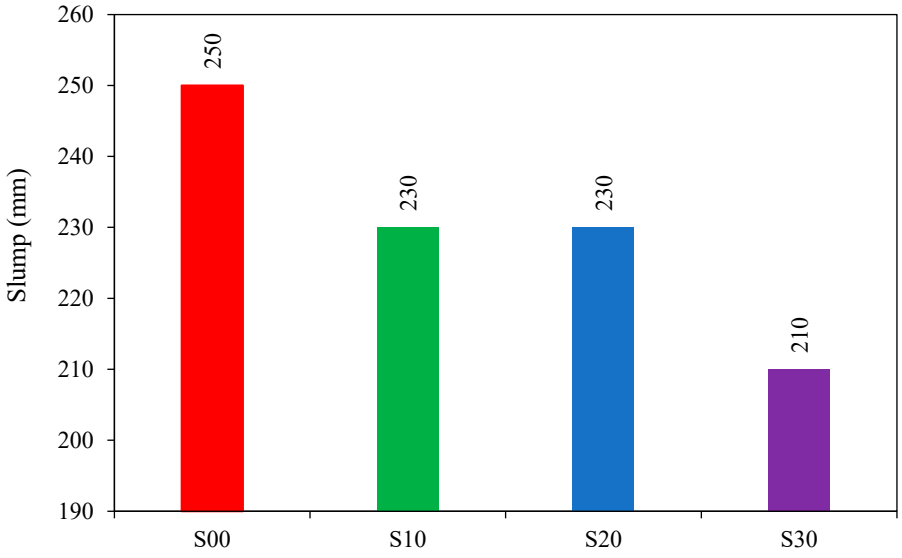

Figure 15. Slump value variation with slag content [16].

Fumed silica is a byproduct of the silicon and ferrosilicon alloy industries. Khater [59] states that due to its spherical shape, adding fumed silica in concrete increases its density and workability. With the activation of sodium silicate, fumed silica can form dihydrogen during synthesis and can be involved in modifying the chemistry and porosity of specimens.

3.1.2. Geopolymer Concrete Setting Time

Setting time refers to the time that concrete can be cast, compacted, and transported [14]. As per ASTM C807 and the British Standards Institution (2009), the Vicat needle device determines the concrete setting time. Antoni et al. [32] observed that NaOH concentration influences the curing time of geopolymer concrete. They noticed that reducing the molarity of NaOH could effectively delay the setting of GPC. Because of the slower reaction rate at a low ambient temperature of 20–24 °C, FA-based geopolymer paste takes more than 24 h to set. However, slag blending considerably reduces both the initial and final setting times. When 10% slag is added to the binder, the initial setting time is lowered to 290 min, further reduced to 95 min, and 40 min when the slag concentration is increased to 20 and 30%. The discrepancy between the beginning and final setting times are reduced by increasing the slag concentration in GPP. As shown in Figure 16, the higher the proportion of slag, the faster the setting. With the rise in slag content, Figure 16 depicts the change in initial and final setting times and the difference in the period between the two. S00, S10, S20, and S30 indicate the addition of 0, 10, 20, and 30% GGBFS blends, respectively [16].

Brew et al. [60] produced quick-setting geopolymer concrete with fumed silica at ambient curing conditions. Waste management can be effectively performed by utilising fumed silica in GPC [61]. The addition of 20–30% fumed silica to geopolymer concrete can improve its setting time [62].

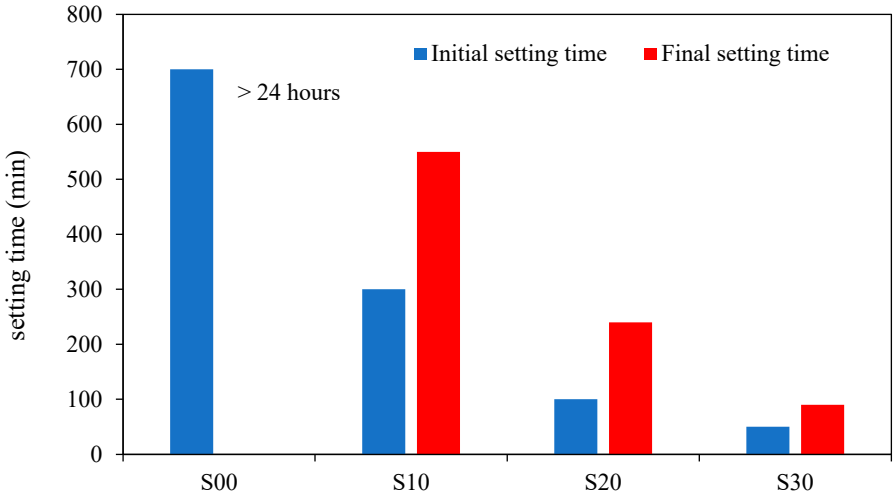

Figure 16. Slag variation during the initial and final setting times [16].

3.2. Mechanical Properties of Hardened Geopolymer Concrete

3.2.1. Compressive Strength

Compressive strength has usually expressed the behaviour of concrete in compression, and the initial elastic modulus represents the strength development with the shape and age of the stress–strain relationship. Lakshmi and Nagan [33] reported that the wet-mixing time, curing time, curing temperature, and particle size influence geopolymer concrete's compressive strength (ASTM C 39). Memon et al. [54] found that geopolymer concrete's compressive strength decreases dramatically when the added water content exceeds 12% of FA mass. After 1 d, heat-cured LCFA-based GPC reaches its maximal compressive strength with no additional increases in compressive strength over time [14]. When cured at 80–90 °C, about 91% of the final strength is formed in just a few hours. Nevertheless, as in PC concrete, GPC cured in an ambient environment setting becomes stronger over time.

All curing regimens (ambient temperature) achieve similar long-term strength findings. The amount of time needed to reach the mixture's maximal compressive strength depends on the curing temperature [14,63]. When employing GPC in the construction of concrete applications subjected to harsh environments, highly high compressive strengths and enhanced durability can be attained [64]. Similar to the relationship between the w/c ratio and the strength of PC concrete, it was found that the ratio of geopolymer particles to water was inversely correlated with the concrete's compressive strength. The entire mass of geopolymer solids [25] is comprised of binder, sodium hydroxide solids, and sodium silicate solids [27]. Ng et al. [65] provided that the ideal mass ratio for compressive strength in a geopolymer combination of fly ash and slag is 35:65. However, this ratio relies on the reactivity of the particular FA and GGBFS utilised. Bhowmick et al. [49] investigated the impact of FA/sand ratio, SiO_2/Na_2O ratio, and water/FA ratio on compressive strength, and according to the findings, the Na_2SiO_3/NaOH ratio has an entirely different impact on GPC compressive strength than the SiO_2/Na_2O ratio. When the Na_2SiO_3/NaOH molar ratio is set at 2.5, there is no significant increase in the compressive strength of GPC. The compressive strength of a structure significantly impacts its stability and safety. The curing conditions and the raw materials impact the compressive strength of FA/GGBS-based geopolymer concrete [66]. Erfanimanesh et al. [45] reported that the zeolite/slag ratio influenced the compressive strength of GPC, as shown in Figure 17. After 7 and 28 days, the GPCs had 30% and 25% higher compressive strengths than the PC concrete. As a result, the mechanical characteristics of the GPC samples were outstanding. Table 3 illustrates the effect of various additives on the behaviour of geopolymer concrete.

Table 3. Effect of different additives on geopolymer concrete compressive strength.

Ref.	Additives	Remarks
Demie, S et al. [67]	Superplasticizer	A high superplasticiser dose increases CS.
Phoo-Ngernkham et al. [68]	Ground granulated BFS	Compressive strength improves when GBFS dosage is increased.
Phoo-Ngernkham et al. [69]	PC mortar	GP composites were developed that have a more uniform and dense structure than concrete.
Islam, A et al. [70]	Ground granulated BFS, palm oil fuel ash	A 67 MPa CS was achieved by combining 30% POFA with 70% GGBS in FA-GP concrete.
Li, Z et al. [71]	Chitosan biopolymer	N-carboxymethyl chitosan's addition greatly enhanced strength and led to a slight boost in compressive strength.
Yang, T et al. [72]	Ground granulated BFS	The CS of GP mixtures can be increased through the addition of slag to the raw material, with a slag/FA dosage ratio of 0.8, resulting in the highest strength.
Rattanasak, U et al. [73]	Sulfate of calcium and sodium, calcium chloride, and sucrose	The final setting time is significantly prolonged by the presence of sugar. As a rule, admixtures boost CS quality.
Nath, S et al. [74]	GBFS, GCS	Partial replacement with GCS yielded a higher CS than partial replacement with GBFS.
Ding, Y.-C [75]	ground granulated BFS	48 MPa CSs were achieved with an M ratio of 0.96 SiO_2/Na_2O and a raw material composition of 70% GGBFS and 30% FA.
Zhang, M et al. [76]	Red mud	There is a decline in CS after 120 days. Safe aggregation of metals where they cannot exceed safe limits.
Kusbiantoro, A et al. [77]	Incinerated rice husk ash	Compressive and bond strength were enhanced when rice husk ash was added at an optimum dosage of 7%.
Torres-Carrasco et al. [78]	Waste glass	Supplemental silicon causes a rise in CS concentration. Typically, 15 g/100 mL is what's prescribed.

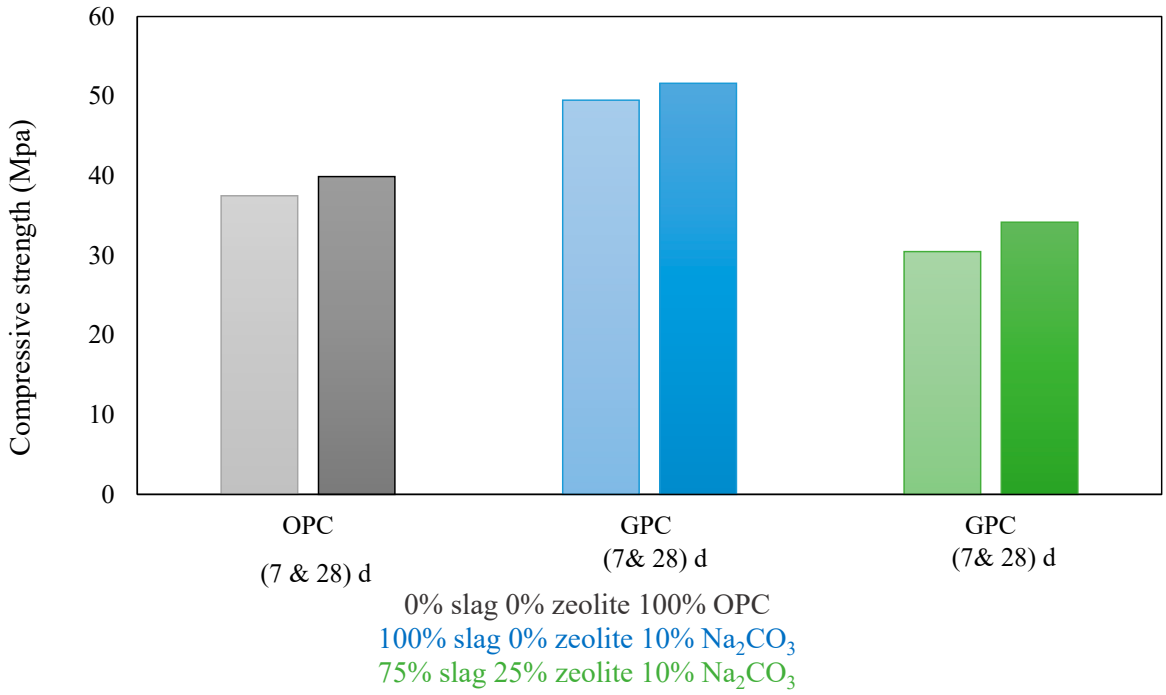

Figure 17. GPC and Portland cement concrete (PCC) compressive strength experiment data (10% Na_2CO_3 by weight of powder mixtures (slag and zeolite), 50% fine aggregate) [45].

3.2.2. Tensile Strength and Flexural Strength

The splitting tensile strength (fsp) and the flexural strength (fr) of GPC increase in tandem with the compressive strength [79], and the compressive strength is proportional to the splitting tensile strength (fsp) and the flexural strength (fr). Test results by Hardijito [63] showed that the splitting tensile strength of geopolymer concrete is only a fraction of the compressive strength. However, there are some deviations from this general response described by some investigators. According to Ryu et al. [14], the rate of tensile strength increase slows as compressive strength increases. Replacing fly ash with GGBS was found to have a lower effect on splitting tensile and flexural strengths as compared with that compressive strength [80]. Tests by Oderji et al. [81] showed a reduction in flexural strength as the fly ash replacement with slag increased from 15% to 20%, knowing that there is a compressive strength enhancement with this modification. Hassan et al. [31] found that in contrast to the elastic modulus of GPC, preheating concrete at 75 °C for 26 h significantly increased compressive and flexural strengths. Other tests by Sarvanan and Elavenil [82] showed that in contrast to the compressive strength if 50% of fly ash is replaced with GGBS, there is a significant splitting tensile strength enhancement. The same observation was made for the elastic modulus property. Comparing data given by Partha et al. [83] with the others showed that using a special heat curing affects enhancing the flexure/compression ratio and, to a lesser degree, the tensile/compression ratio, as compared with the case of ambient temperature curing. Lee et al. [84] presented the tensile strength of the GPC experimental test was measured at 7, 14, and 28 days. Figure 18 demonstrates that when the ratio of sand to FA increases, the tensile strength steadily falls. The outcomes of experimental tests of geopolymer concrete tensile strength were compared by Zhuang et al. [85] based on the design strength of the ACI code, and findings suggest that the splitting tensile strength of GPC is comparable to that of the ACI design. According to Zhuang et al. [85], the tensile strength of the GPC was better than that of PC-quality concrete.

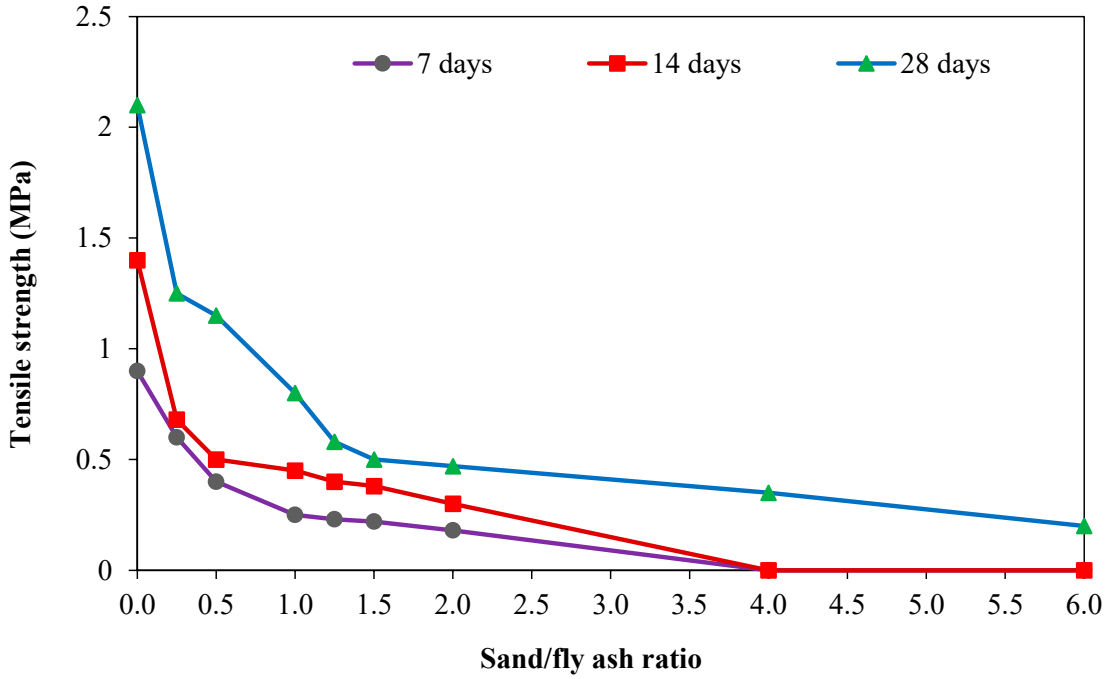

Figure 18. GPC tensile strength of different sand/fly ash ratios [84].

3.3. Microstructural Properties of Hardened GPC

3.3.1. X-ray Diffraction (XRD)

X-ray diffraction is a microstructural scanning test performed to investigate and identify a material's atomic and crystallographic nature. The XRD analysis test involves the irradiation of materials with entrant X-rays and then counting the intensities and scattering angles at which X-rays are emitted; the dispersed rays are expressed in terms of scattering angles, which examines the position of the substance to identify its composition, and identifies scattered intensity peaks. XRD is used in conjunction with other microstructural analyses such as optical light microscopy, electron microprobe microscopy, and scanning electron microscopy in geologic research, mainly if the sample to be analysed is a mixture; XRD data can identify each mineral in a sample and its concentration.

Different researchers have studied the XRD pattern of geopolymer concrete [66,84–95]. Al Bakri et al. [95] noticed that "The basic material of the geopolymer-concrete is of a prevailingly amorphous character only seldom containing needle-shaped minority crystals". Figure 19 shows the X-ray diffraction (XRD) geopolymer concrete in its as-received condition.

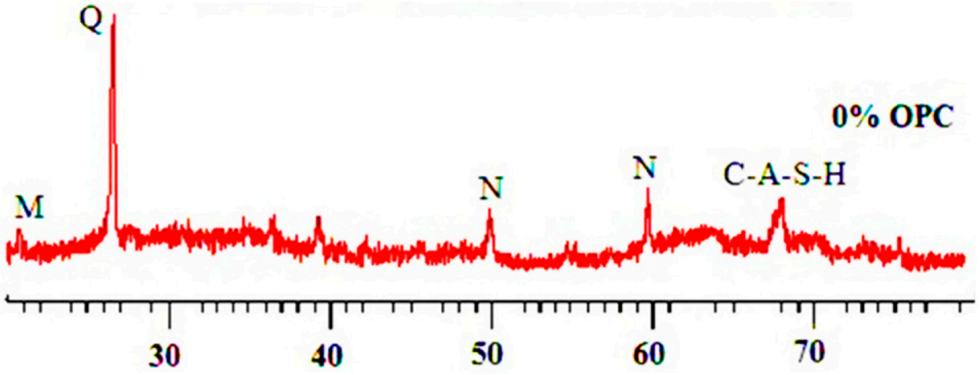

Figure 19. XRD of geopolymer concrete [86].

3.3.2. Scanning Electron Micrograph (SEM) and Energy Dispersive X-ray (EDX)

SEM involves examining and scanning the material's surface with a focused beam of electrons through image analysis to measure and assess fine details. When electrons contact sample atoms, they provide multiple surface topography and composition signals, highlighting component failures, detecting particles, and analysing the interactions between substances and substrates.

Some studies have investigated the SEM and EDX test of GPC [88,96–99]. The microstructure of geopolymer-treated concrete appears more refined and denser than untreated concrete (Figure 20). Calcium hydroxide was not detected using EDX, but particles of non-reactant lime were present at levels similar to the control specimen. The main component of geopolymer cement is lime, which explains why it has these properties. Calcium, silicon, magnesium, and potassium peaks increase dramatically in the EDX elemental analysis of the geopolymer-modified PC concrete, which can be attributed to the high concentrations of these elements in the geopolymer cement (except potassium, which originates mostly from the alkaline activator).

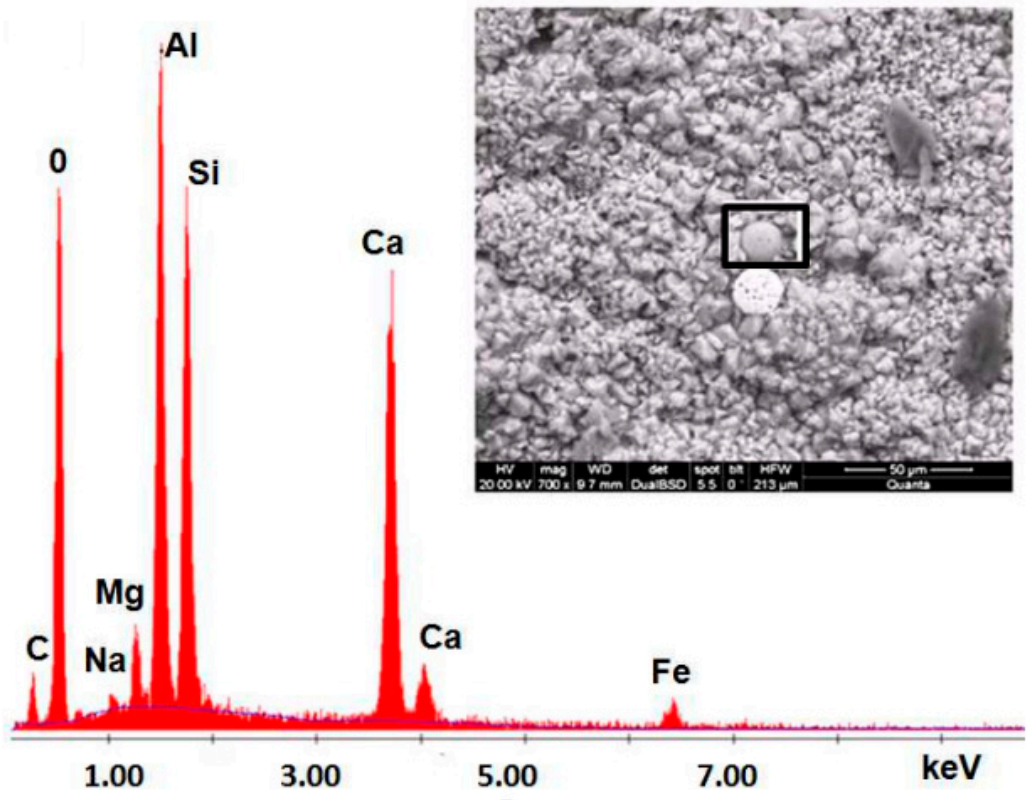

Figure 20. SEM and EDX curve showing the chemical composition of geopolymer concrete [99].

Jittabut et al. [88] showed that scanning electron microscopy (SEM) pictures of the failed specimens were taken to investigate the geopolymer concrete microstructure. Figure 21 shows the micrographs of geopolymer concrete. The microstructure revealed that several phases exist in the matrix GPC. According to Han et al. [90], the microstructure investigation is absolute, thick, and unbroken, with a highly reactive microstructure. The polymerisation results were in good condition, with no breakdown or crystalline water.

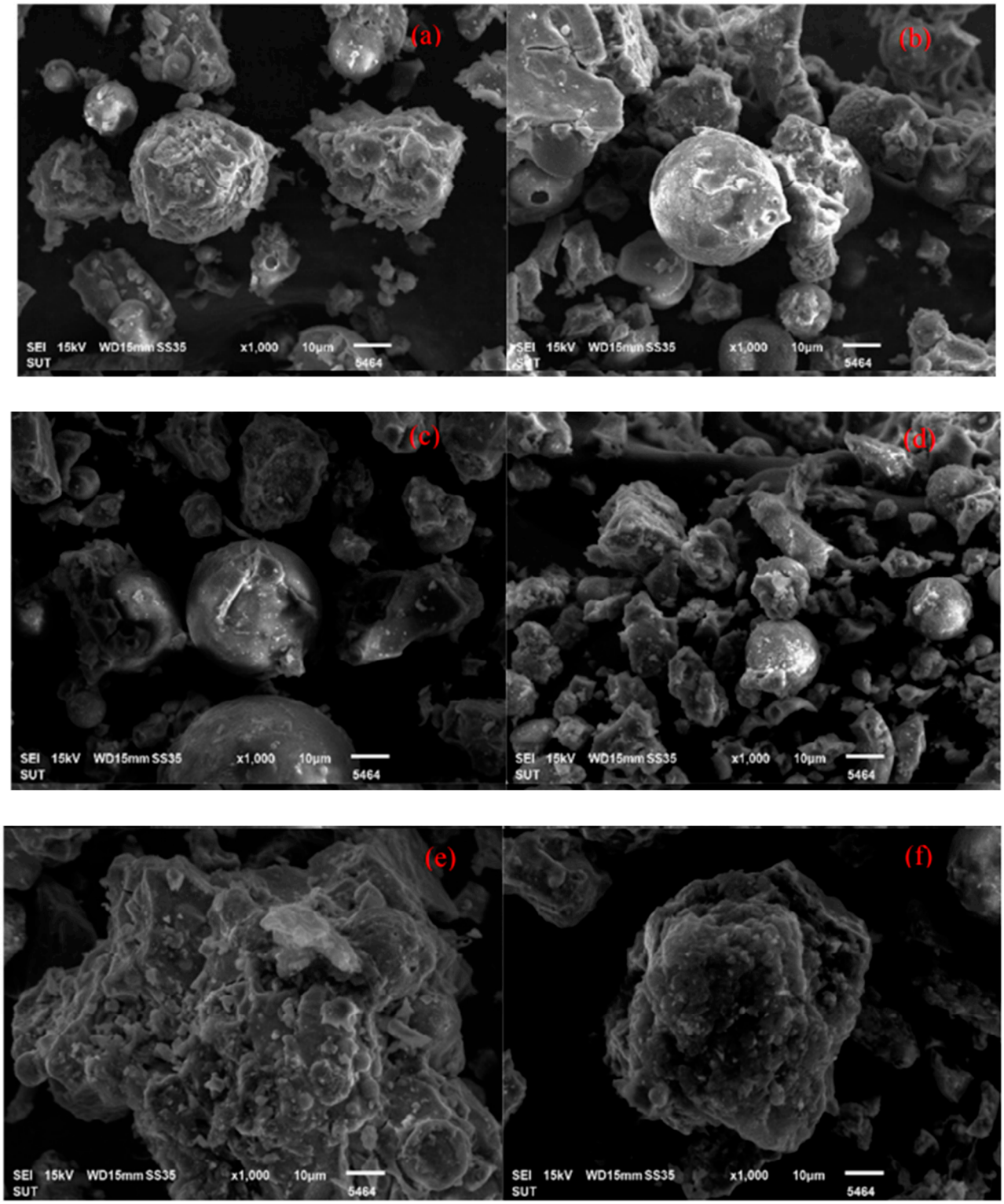

Figure 21. SEM images of a fracture surface of geopolymer nano-composite reinforced with carbon nanotubes (**a**) NaOH 10M control without MWCNTs (**b**) 10M control with CNTs 1 wt% (**c**) NaOH 15M control without MWCNTs (**d**) 15M control with MWCNTs 1 wt% (**e**) NaOH 20Mcontrol without MWCNTs and (**f**) 20M control with MWCNTs 1 wt%. [88].

3.3.3. Fourier Transform Infrared Spectroscopy (FTIR)

FTIR techniques are used to measure the infrared absorption, emission, and photo-conductivity of a solid, liquid, or gas and identify PHB functional categories. Very limited

studies have investigated the FTIR test of GPC [100–102]. Figure 22 represents the curing geopolymer sample spectra in the range of 4000 and 400 cm^{-1}. Rajini et al. [102] observed that the broad bands in geopolymer mixtures at roughly 3350–3370 cm^{-1} are caused by the tensile vibrations of H-O-H bonds, whereas the broad bands at 1640–1646 cm^{-1} are caused by the bending vibration of the water-associated-OH group.

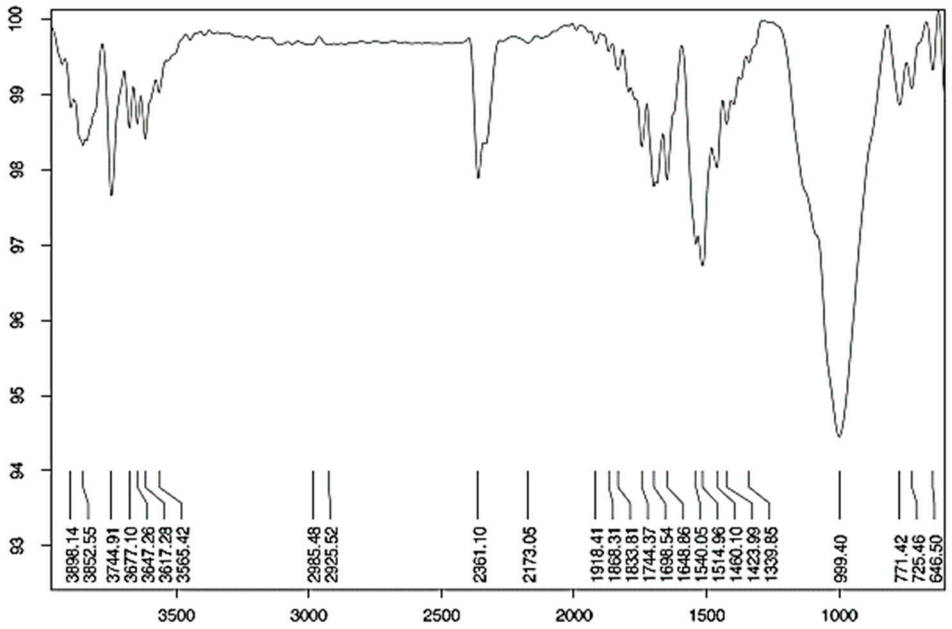

Figure 22. Fourier transform infrared spectroscopy (FTIR) of geopolymer concrete [102].

Salih, M. A. et al. [101] explain that "the spectra of raw geopolymer paste with different sodium silicate to sodium hydroxide ratios were distinguished with six groups of bands in the regions of 750–850 cm^{-1}, 900–1200 cm^{-1}, 1200–1300 cm^{-1}, 1300–1600 cm^{-1}, 1600–1700 cm^{-1}, and 2850–3700 cm^{-1} (Figure 23). The first peak was observed at a wave number of 750–850 cm^{-1} centred at 783 cm^{-1}, which may refer to the symmetric stretching vibration of Si–O–Si".

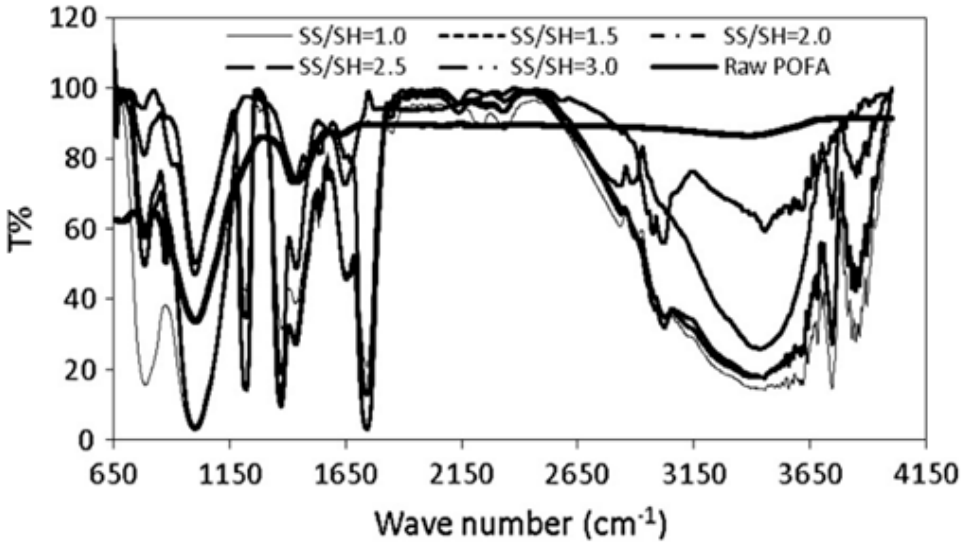

Figure 23. FTIR spectra of raw geopolymerized [101].

3.3.4. Differential Scanning Calorimetry (DSC)

DSC is an impressive scientific tool for pointing out various physical properties and thermal transitions of polymeric materials. Several distinctive features of the geopolymer pastes can be measured with DSC, which allows observation of exothermic and endothermic processes, in addition to glass transition temperatures (Tg).

Different researchers have studied the DSC analysis of geopolymer concrete [103–107]. Jamil, N. H. et al. [107] showed the geopolymer's range of thermograms (exothermal up) (Figure 24), where the geopolymer demonstrates some peaks in the matrix.

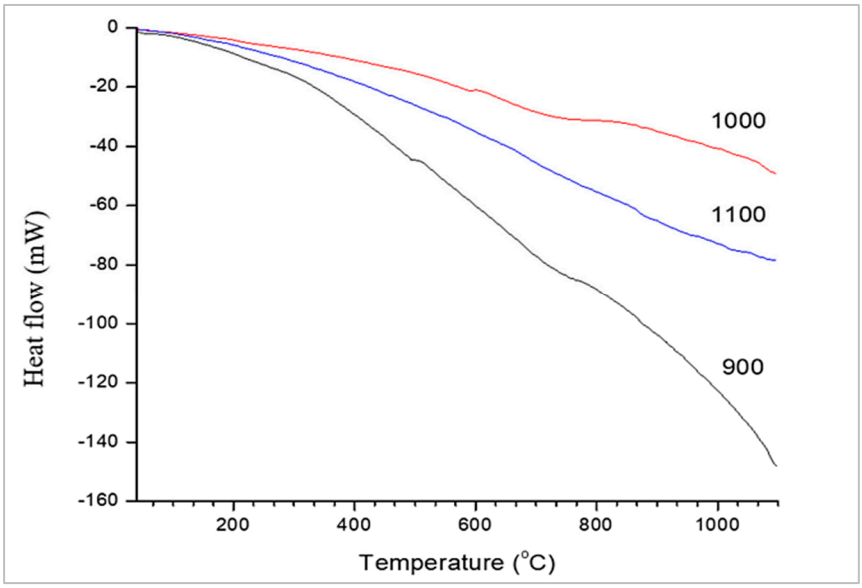

Figure 24. Differential scanning calorimetry (DSC) [107].

Figure 25 depicts the differential scanning calorimetry (DSC) thermograms of geopolymer paste after 28 days, which are similar to the results reported in previous works [101]. From what can be seen in the diagram, there was only one discernible endothermic peak. The pastes with 1:1, 1:1.5, 2:1, 2:1, and 3:1 sodium silicate to sodium hydroxide ratios had this major peak centred at 117.55 C, 114.49 C, 119.40 C, 121.42 C, and 120.02 C, respectively. Water being released from partially dehydrated C-S-H clusters may account for the peaks. For stoichiometric ratios of 1.0, 1.5, 2.0, 2.5, and 3.0 between sodium silicate and sodium hydroxide, the endothermic results were 3888.03, 3,43.106, 3,84.209, 5140.29, and 7410.29 W/g, respectively.

3.3.5. Thermal Gravimetric Analysis (TGA)

TGA aids in the identification of several concrete phases, including calcite, portlandite, C-A-H, C-A-S-H, etc. The hydration reaction is often checked by measuring the CH content; if the CH level decreases, it indicates that CH has been consumed in the hydration reaction. Researchers from several fields have examined the geopolymer concrete TGA [108–111].

Figure 26 shows the TGA analysis of geopolymer concrete's thermogram. Rosas-Casarez et al. [94] emphasised the primary drop in slope between 0 °C and 1000 °C. In the temperature range of 0 to 120 °C, the dewatering operation resulted in a ten percent weight loss, which is the first substantial drop (number 1 in Figure 26). This process is related to free water that has been adsorbed on the sample's surface, water that can evaporate from the sample, and the sample's porosity. However, a current study on the loss of hydrated sodium aluminosilicate gel contradicts this notion. Between 120 and 200 °C, the presence of NASH gel contributes significantly to heat degradation (number 2 in Figure 26). Carbonate loss in mass between 450 and 800 °C may be attributable to carbonates synthesised in the outside environment (number 3 in Figure 26). This method

can be used as a comparative method between materials [112–117] by relating the water binding capacity for each compound against the effect of temperature. This allows for the differentiation and probing of structural variants and the presence of compounds in a material.

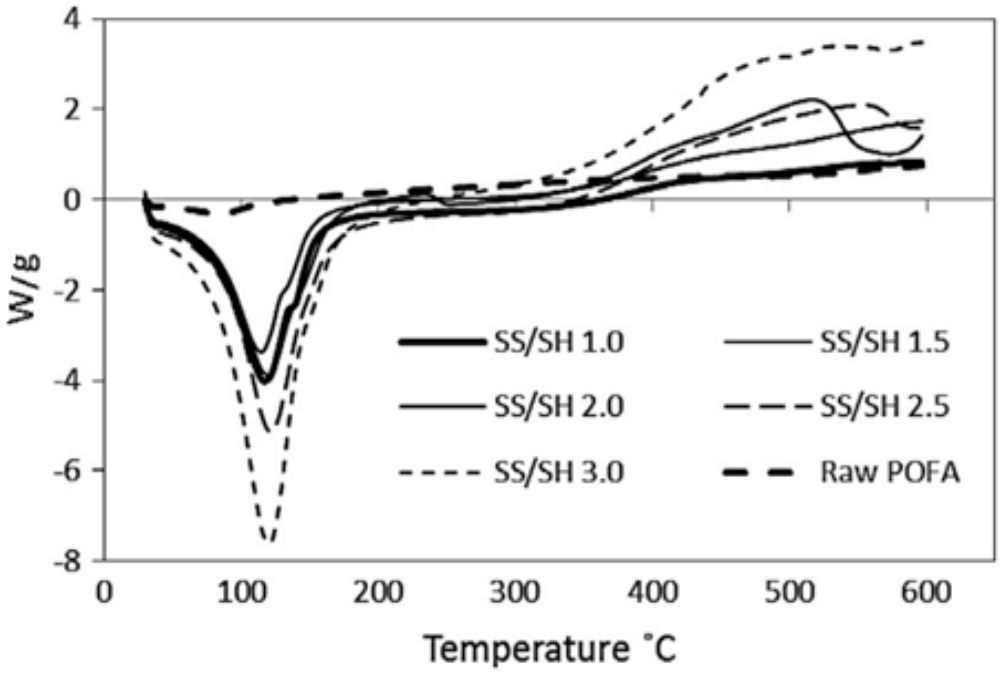

Figure 25. DSC diagrams of raw geopolymerized [101].

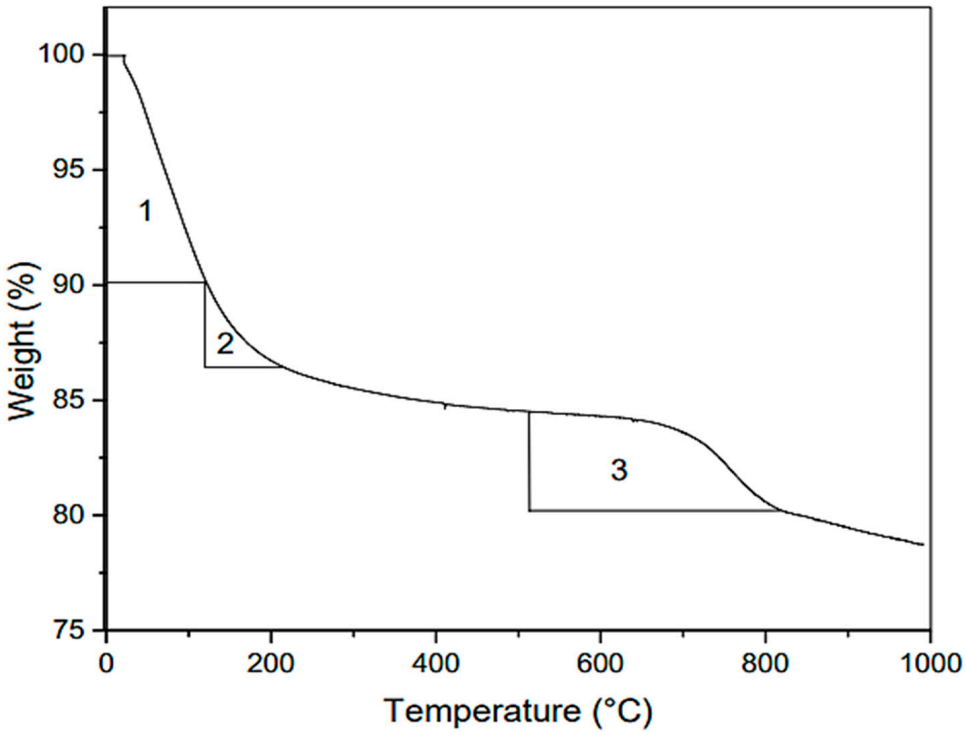

Figure 26. Thermogravimetric (TGA) analysis of geopolymer [94].

4. Scope and Future Research Work

Geopolymer concrete offers much potential in the construction industry. Even though geopolymer concrete has been researched very well in the last few years, several aspects should be covered, and extended data should be collected to understand the behaviour of geopolymer concrete before introducing it to the construction sector. The large-scale structural elements of GPC and the performance of reinforced geopolymer concrete should be investigated. Moreover, the behaviour of geopolymer materials in an aggressive environment, such as a marine environment, must be studied.

Research studies available on structural members of GPC are still lacking. Thus, more investigations need to be carried out on the structural behaviour under the different loading states, and proper modelling is essential, such as developing a proper relationship between the flexural strength, compressive strength, shear strength, and modulus of elasticity of GPC. Moreover, the elasticity and plasticity of geopolymer materials should be well studied to help structural engineers when they are designing buildings. Based on fundamental research, embarking on solid wastes to explore the preparation of varied characteristics of geopolymers in order to produce high-value-added application domains should be one of the primary paths of future geopolymer research development [91,92,111–132].

5. Conclusions

The mechanical properties and microstructural characteristics of geopolymer concrete were reviewed. From the above literature, the following are the final thoughts, along with suggestions for more research:

- Construction with geopolymer concrete is more durable and stronger than with PC concrete;
- Many factors, including curing conditions, the ratio of alkaline to the binder, and the type of activator, have an important impact on the mechanical properties of geopolymer concrete. Consequently, a proper mix design is required to achieve the target strength;
- Geopolymer concrete possesses all the potential characteristics for future applications in civil engineering because it is a green material and requires strength and durability properties for all types of projects in the construction industry;
- Even though it is known that GPC could be used as a replacement material and is a cleaner and more sustainable form of concrete, it is still not widely used in construction;
- Geopolymer concrete needs a standard code to be used more often in building structures;
- In terms of mechanical and microstructural performance, geopolymer concrete was better than PC concrete, especially after exposure to high temperatures;
- The effect of using geopolymer as a partial replacement for PC on the microstructure can be easily noticed; the microstructure has become significantly denser and more homogenous compared with the control specimen, while the number of voids has decreased;
- C-S-H gel and geopolymer gel enhance the mechanical and microstructural properties of precursors that are either high in Ca or contain a combination of Ca components.

Author Contributions: Conceptualisation, A.S., A.H., H.M.N., S.Q., M.M.S.S. and N.S.M.; methodology, A.S., A.H., H.M.N., M.M.S.S. and N.S.M.; software, A.S. and A.H.; validation, H.M.N., S.Q., M.M.S.S. and N.S.M.; formal analysis, A.S. and A.H.; investigation, A.S., A.H., H.M.N., S.Q., M.M.S.S. and N.S.M.; resources, A.S., A.H., H.M.N., M.M.S.S., N.S.M. and K.A.; data curation, A.S., A.H., H.M.N., M.M.S.S., S.Q., K.A. and N.S.M.; writing—original draft preparation, A.S. and A.H.; writing—review and editing, A.H., H.M.N., M.M.S.S. and N.S.M.; visualisation, A.S. and A.H.; supervision, A.S., A.H. and H.M.N.; project administration, M.M.S.S.; funding acquisition, M.M.S.S. All authors have read and agreed to the published version of the manuscript.

Funding: The research is partially funded by the Ministry of Science and Higher Education of the Russian Federation under the strategic academic leadership program "Priority 2030" (Agreement 075-15-2021-1333 dated 30 September 2021).

Institutional Review Board Statement: Not applicable.

Informed Consent Statement: Not applicable.

Data Availability Statement: Not applicable.

Acknowledgments: The authors extend their thanks to the Ministry of Science and Higher Education of the Russian Federation for funding this work.

Conflicts of Interest: The authors declare no conflict of interest.

References

1. Amran, Y.M.; Alyousef, R.; Alabduljabbar, H.; El-Zeadani, M. Clean production and properties of geopolymer concrete; A review. *J. Clean. Prod.* **2020**, *251*, 119679. [CrossRef]
2. Basha, S.M.; Reddy, C.B.; Vasugi, K. Strength behaviour of geopolymer concrete replacing fine aggregates by M-sand and E-waste. *Int. J. Eng. Trends Technol.* **2016**, *40*, 401–407. [CrossRef]
3. Bhutta, A.; Farooq, M.; Zanotti, C.; Banthia, N. Pull-out behavior of different fibers in geopolymer mortars: Effects of alkaline solution concentration and curing. *Mater. Struct.* **2017**, *50*, 80. [CrossRef]
4. Castel, A.; Foster, S.; Ng, T.; Sanjayan, J.; Gilbert, R. Creep and drying shrinkage of a blended slag and low calcium fly ash geopolymer Concrete. *Mater. Struct.* **2016**, *49*, 1619–1628. [CrossRef]
5. Ahmed, H.U.; Mahmood, L.J.; Muhammad, M.A.; Faraj, R.H.; Qaidi, S.M.A.; Sor, N.H.; Mohammed, A.S.; Mohammed, A.A. Geopolymer concrete as a cleaner construction material: An overview on materials and structural performances. *Clean. Mater.* **2022**, *5*, 100111. [CrossRef]
6. Qaidi, S.M.A.; Tayeh, B.A.; Isleem, H.F.; de Azevedo, A.R.G.; Ahmed, H.U.; Emad, W. Sustainable utilisation of red mud waste (bauxite residue) and slag for the production of geopolymer composites: A review, Case Studies in Construction. *Materials* **2022**, *16*, e00994.
7. IEA. *Global Cement Production, 2010–2019*; IEA: Paris, France, 2020.
8. Chowdhury, S.; Mohapatra, S.; Gaur, A.; Dwivedi, G.; Soni, A. Study of various properties of geopolymer concrete–A review. *Mater. Today Proc.* **2021**, *46*, 5687–5695. [CrossRef]
9. Mohajerani, A.; Suter, D.; Jeffrey-Bailey, T.; Song, T.; Arulrajah, A.; Horpibulsuk, S.; Law, D. Recycling waste materials in geopolymer concrete. *Clean Technol. Environ. Policy* **2019**, *21*, 493–515. [CrossRef]
10. Ahmed, H.U.; Mohammed, A.S.; Qaidi, S.M.A.; Faraj, R.H.; Sor, N.H.; Mohammed, A.A. Compressive strength of geopolymer concrete composites: A systematic comprehensive review, analysis and modeling. *Eur. J. Environ. Civ. Eng.* **2022**, 1–46. [CrossRef]
11. Ahmed, S.N.; Sor, N.H.; Ahmed, M.A.; Qaidi, S.M.A. Thermal conductivity and hardened behavior of eco-friendly concrete incorporating waste polypropylene as fine aggregate. *Mater. Today Proc.* **2022**, *57*, 818–823. [CrossRef]
12. Aslam, F.; Zaid, O.; Althoey, F.; Alyami, S.H.; Qaidi, S.M.A.; de Prado Gil, J.; Martínez-García, R. Evaluating the influence of fly ash and waste glass on the characteristics of coconut fibers reinforced concrete. *Struct. Concr.* **2022**. [CrossRef]
13. Davidovits, J. Geopolymers. *J. Therm. Anal.* **1991**, *37*, 1633–1656. [CrossRef]
14. Ryu, G.S.; Lee, Y.B.; Koh, K.T.; Chung, Y.S. The mechanical properties of fly ash-based geopolymer concrete with alkaline activators. *Constr. Build. Mater.* **2013**, *47*, 409–418. [CrossRef]
15. Sreevidya, V. Investigations on the Flexural Behaviour of Ferro Geopolymer Composite Slabs. 2014. Available online: https://www.researchgate.net/publication/321050166_INVESTIGATIONS_ON_THE_FLEXURAL_BEHAVIOUR_OF_FERRO_GEOPOLYMER_COMPOSITE_SLABS (accessed on 1 September 2022).
16. Davidovits, J. False values on CO_2 emission for geopolymer cement/concrete published in scientific papers. *Tech. Pap.* **2015**, *24*, 1–9.
17. Gollakota, A.R.K.; Volli, V.; Shu, C.-M. Progressive utilisation prospects of coal fly ash: A review. *Sci. Total Environ.* **2019**, *672*, 951–989. [CrossRef] [PubMed]
18. Xiao, R.; Polaczyk, P.; Zhang, M.; Jiang, X.; Zhang, Y.; Huang, B.; Hu, W. Evaluation of glass powder-based geopolymer stabilised road bases containing recycled waste glass aggregate. *Transp. Res. Rec.* **2020**, *2674*, 22–32. [CrossRef]
19. Assi, L.; Carter, K.; Deaver, E.; Anay, R.; Ziehl, P. Sustainable concrete: Building a greener future. *J. Clean. Prod.* **2018**, *198*, 1641–1651. [CrossRef]
20. Assi, L.N.; Carter, K.; Deaver, E.; Ziehl, P. Review of availability of source materials for geopolymer/sustainable concrete. *J. Clean. Prod.* **2020**, *263*, 121477. [CrossRef]
21. van Jaarsveld, J.G.S.; van Deventer, J.S.J.; Lukey, G.C. The characterisation of source materials in fly ash-based geopolymers. *Mater. Lett.* **2003**, *57*, 1272–1280. [CrossRef]
22. Ahmad, J.; Majdi, A.; Elhag, A.B.; Deifalla, A.F.; Soomro, M.; Isleem, H.F.; Qaidi, S. A Step towards Sustainable Concrete with Substitution of Plastic Waste in Concrete: Overview on Mechanical, Durability and Microstructure Analysis. *Crystals* **2022**, *12*, 944. [CrossRef]
23. Ahmed, H.U.; Mohammed, A.A.; Rafiq, S.; Mohammed, A.S.; Mosavi, A.; Sor, N.H.; Qaidi, S.M.A. Compressive Strength of Sustainable Geopolymer Concrete Composites: A State-of-the-Art Review. *Sustainability* **2021**, *13*, 13502. [CrossRef]

24. Ahmed, H.U.; Mohammed, A.S.; Faraj, R.H.; Qaidi, S.M.A.; Mohammed, A.A. Compressive strength of geopolymer concrete modified with nano-silica: Experimental and modeling investigations. *Case Stud. Constr. Mater.* **2022**, *16*, e01036. [CrossRef]
25. Hassan, A.; Arif, M.; Shariq, M. Use of geopolymer concrete for a cleaner and sustainable environment–A review of mechanical properties and microstructure. *J. Clean. Prod.* **2019**, *223*, 704–728. [CrossRef]
26. Qaidi, S.M.A.; Atrushi, D.S.; Mohammed, A.S.; Ahmed, H.U.; Faraj, R.H.; Emad, W.; Tayeh, B.A.; Najm, H.M. Ultra-high-performance geopolymer concrete: A review. *Constr. Build. Mater.* **2022**, *346*, 128495. [CrossRef]
27. Hassan, A.; Arif, M.; Shariq, M. A review of properties and behaviour of reinforced geopolymer concrete structural elements-A clean technology option for sustainable development. *J. Clean. Prod.* **2020**, *245*, 118762. [CrossRef]
28. Habert, G.; D'Espinose De Lacaillerie, J.B.; Roussel, N. An Environmental Evaluation of Geopolymer Based Concrete Production: Reviewing Current Research Trends. *J. Clean. Prod.* **2011**, *19*, 1229–1238. [CrossRef]
29. Umniati, B.S.; Risdanareni, P.; Zein, F.T.Z. Workability Enhancement of Geopolymer Concrete through the Use of Retarder. *AIP Conf. Proc.* **2017**, *1887*, 020033.
30. Mehta, A.; Siddique, R. Properties of Low-Calcium Fly Ash Based Geopolymer Concrete Incorporating PC as Partial Re-placement of Fly Ash. *Constr. Build. Mater.* **2017**, *150*, 792–807. [CrossRef]
31. Hassan, A. Experimental Study of Fly Ash Based Geopolymer Concrete. *Int. J. Adv. Earth Sci. Eng.* **2018**, *7*, 635–648. [CrossRef]
32. Antoni, P.; Satria, J.; Sugiarto, A.; Hardjito, D. Effect of Variability of Fly Ash Obtained from the Same Source on the Characteristics of Geopolymer. *MATEC Web Conf.* **2017**, *97*, 01026. [CrossRef]
33. Lakshmi, R.; Nagan, S. Utilization of Waste e Plastic Particles in Cementitious Mixtures. *J. Struct. Eng. (Madras)* **2011**, *38*, 26–35.
34. Memon, F.A.; Nuruddin, M.F.; Demie, S.; Shafiq, N. Effect of Superplasticizer and Extra Water on Workability and Com-pressive Strength of Self-Compacting Geopolymer Concrete. *Res. J. Appl. Sci. Eng. Technol.* **2012**, *4*, 407–414.
35. Warid Wazien, A.Z.; Al Bakri Abdullah, M.M.; Abd Razak, R.; Mohd Remy Rozainy, M.A.Z.; Mohd Tahir, M.F.; Hussin, K. Potential of Geopolymer Mortar as Concrete Repairing Materials. *Mater. Sci. Forum* **2016**, *857*, 382–387. [CrossRef]
36. Sathonsaowaphak, A.; Chindaprasirt, P.; Pimraksa, K. Workability and Strength of Lignite Bottom Ash Geopolymer Mortar. *J. Hazard. Mater.* **2009**, *168*, 44–50. [CrossRef] [PubMed]
37. Chindaprasirt, P.; Chareerat, T.; Sirivivatnanon, V. Workability and Strength of Coarse High Calcium Fly Ash Geopolymer. *Cem. Concr. Compos.* **2007**, *29*, 224–229. [CrossRef]
38. *ASTM C 1437-07*; Standard Test Methods for Flow of Hydraulic Cement Mortar. ASTM International: West Conshohocken, PA, USA, 2008.
39. Bhowmick, A.; Ghosh, S. Effect of Synthesising Parameters on Workability and Compressive Strength of Fly Ash Based Geopolymer Mortar. *Int. J. Struct. Civ. Eng.* **2012**, *3*, 168–177.
40. *ASTM C1437-01*; Standard Test Method for Flow of Hydraulic Cement Mortar. ASTM International: West Conshohocken, PA, USA, 2001.
41. *BS EN 480-5*; Admixtures for Concrete, Mortar and Grout—Test Methods Part 5: Determination of Capillary Absorption. British Standard Institute: London, UK, 2005; Volume 3, pp. 480–485.
42. Jumrat, S.; Chatveera, B.; Rattanadecho, P. Dielectric Properties and Temperature Profile of Fly Ash-Based Geopolymer Mortar. *Int. Commun. Heat Mass Transf.* **2011**, *38*, 242–248. [CrossRef]
43. Saloma; Saggaff, A.; Hanafiah; Mawarni, A. Geopolymer Mortar with Fly Ash. *MATEC Web Conf.* **2016**, *78*, 01026. [CrossRef]
44. Phoo-ngernkham, T.; Sata, V.; Hanjitsuwan, S.; Ridtirud, C.; Hatanaka, S.; Chindaprasirt, P. Compressive Strength, Bending and Fracture Characteristics of High Calcium Fly Ash Geopolymer Mortar Containing Portland Cement Cured at Ambient Temperature. *Arab. J. Sci. Eng.* **2016**, *41*, 1263–1271. [CrossRef]
45. Erfanimanesh, A.; Sharbatdar, M.K. Mechanical and Microstructural Characteristics of Geopolymer Paste, Mortar, and Concrete Containing Local Zeolite and Slag Activated by Sodium Carbonate. *J. Build. Eng.* **2020**, *32*, 101781. [CrossRef]
46. Yusuf, T.O.; Ismail, M.; Usman, J.; Noruzman, A.H. Impact of Blending on Strength Distribution of Ambient Cured Me-takaolin and Palm Oil Fuel Ash Based Geopolymer Mortar. *Adv. Civ. Eng.* **2014**, *2014*, 658067. [CrossRef]
47. Ismail, M.; Yusuf, T.O.; Noruzman, A.H.; Hassan, I.O. Early Strength Characteristics of Palm Oil Fuel Ash and Metakaolin Blended Geopolymer Mortar. *Adv. Mater. Res.* **2013**, *690*, 1045–1048. [CrossRef]
48. De Rossi, A.; Ribeiro, M.J.; Labrincha, J.A.; Novais, R.M.; Hotza, D.; Moreira, R.F.P.M. Effect of the Particle Size Range of Construction and Demolition Waste on the Fresh and Hardened-State Properties of Fly Ash-Based Geopolymer Mortars with Total Replacement of Sand. *Process Saf. Environ. Prot.* **2019**, *129*, 130–137. [CrossRef]
49. Cyr, M.; Idir, R.; Poinot, T. Properties of Inorganic Polymer (Geopolymer) Mortars Made of Glass Cullet. *J. Mater. Sci.* **2012**, *47*, 2782–2797. [CrossRef]
50. Huseien, G.F.; Mirza, J.; Ismail, M.; Hussin, M.W. Influence of Different Curing Temperatures and Alkali Activators on Properties of GBFS Geopolymer Mortars Containing Fly Ash and Palm-Oil Fuel Ash. *Constr. Build. Mater.* **2016**, *125*, 1229–1240. [CrossRef]
51. Steinerova, M. Mechanical Properties of Geopolymer Mortars in Relation to Their Porous Structure. *Ceram. Silik.* **2011**, *55*, 362–372.
52. Li, X.; Wang, Z.; Jiao, Z. Influence of Curing on the Strength Development of Calcium-Containing Geopolymer Mortar. *Materials* **2013**, *6*, 5069–5076. [CrossRef]

53. Atiş, C.D.; Görür, E.B.; Karahan, O.; Bilim, C.; Ilkentapar, S.; Luga, E. Very High Strength (120 MPa) Class F Fly Ash Ge-opolymer Mortar Activated at Different NaOH Amount, Heat Curing Temperature and Heat Curing Duration. *Constr. Build. Mater.* **2015**, *96*, 673–678. [CrossRef]
54. Al-Majidi, M.H.; Lampropoulos, A.; Cundy, A.; Meikle, S. Development of Geopolymer Mortar under Ambient Temper-ature for in Situ Applications. *Constr. Build. Mater.* **2016**, *120*, 198–211. [CrossRef]
55. Wongsa, A.; Kunthawatwong, R.; Naenudon, S.; Sata, V.; Chindaprasirt, P. Natural Fiber Reinforced High Calcium Fly Ash Geopolymer Mortar. *Constr. Build. Mater.* **2020**, *241*, 118143. [CrossRef]
56. Lloyd, N.A.; Rangan, B.V. Geopolymer Concrete with Fly Ash. In Proceedings of the 2nd International Conference on Sustainable Construction Materials and Technologies, Ancona, Italy, 28–30 June 2010.
57. Patil, S.; Karikatti, V.; Chitawadagi, M. Granulated Blast-Furnace Slag (GGBS) based Geopolymer Concrete–Review. *Int. J. Adv. Sci. Eng.* **2018**, *5*, 879–885. [CrossRef]
58. Rajarajeswari, A.; Dhinakaran, G. Compressive strength of GGBFS based GPC under thermal curing. *Constr. Build. Mater.* **2016**, *126*, 552–559. [CrossRef]
59. Khater, H.M. Efect of fumed silica on the characterisation of the geopolymer materials. *Int. J. Adv. Struct. Eng.* **2013**, *5*, 12. [CrossRef]
60. Brew, D.R.M.; MacKenzie, K.J.D. Geopolymer synthesis using fumed silica and sodium aluminate. *J. Mater. Sci.* **2007**, *42*, 3990–3993. [CrossRef]
61. Bajpai, R.; Kailash, C.; Anshuman, S.; Kuldip, S.S.; Manpreet, S. Environmental impact assessment of fy ash and silica fume based geopolymer concrete. *J. Clean. Prod.* **2020**, *254*, 120147. [CrossRef]
62. Liu, Y.; Shi, C.; Zhang, Z.; Li, N.; Shi, D. Mechanical and fracture properties of ultra-high performance geopolymer concrete: Efects of steel fber and silica fume. *Cem. Concr. Compos.* **2020**, *112*, 103665. [CrossRef]
63. Rangan, B.; Hardjito, D. Studies on Fly Ash-Based Geopolymer Concrete. Ph.D. Thesis, Curtin University of Technology, Bentley, Australia, 2005.
64. Day, K.W. Properties of Concrete. In *Concrete Mix Design, Quality Control and Specification*; CRC Rress: Boca Raton, FL, USA, 2021.
65. Ng, T.S.; Foster, S.J. Development of High Performance Geopolymer Conscrete. In Proceedings of the Futures in Mechanics of Structures and Materials—20th Australasian Conference on the Mechanics of Structures and Materials (ACMSM20), Toowoomba, Australia, 2–5 November 2008.
66. Le, H.T.N.; Poh, L.H.; Wang, S.; Zhang, M.H. Critical Parameters for the Compressive Strength of High-Strength Concrete. *Cem. Concr. Compos.* **2017**, *82*, 202–216. [CrossRef]
67. Demie, S.; Nuruddin, M.F.; Shafiq, N. Effects of micro-structure characteristics of interfacial transition zone on the compressive strength of self-compacting geopolymer concrete. *Constr. Build. Mater.* **2013**, *41*, 91–98. [CrossRef]
68. Phoo-Ngernkham, T.; Maegawa, A.; Mishima, N.; Hatanaka, S.; Chindaprasirt, P. Effects of sodium hydroxide and sodium silicate solutions on compressive and shear bond strengths of FA–GBFS geopolymer. *Constr. Build. Mater.* **2015**, *91*, 1–8. [CrossRef]
69. Phoo-Ngernkham, T.; Sata, V.; Hanjitsuwan, S.; Ridtirud, C.; Hatanaka, S.; Chindaprasirt, P. High calcium fly ash geopolymer mortar containing Portland cement for use as repair material. *Constr. Build. Mater.* **2015**, *98*, 482–488. [CrossRef]
70. Islam, A.; Alengaram, U.J.; Jumaat, M.Z.; Bashar, I.I. The development of compressive strength of ground granulated blast furnace slag-palm oil fuel ash-fly ash based geopolymer mortar. *Mater. Des.* **2014**, *56*, 833–841. [CrossRef]
71. Li, Z.; Chen, R.; Zhang, L. Utilization of chitosan biopolymer to enhance fly ash-based geopolymer. *J. Mater. Sci.* **2013**, *48*, 7986–7993. [CrossRef]
72. Yang, T.; Yao, X.; Zhang, Z.; Wang, H. Mechanical property and structure of alkali-activated fly ash and slag blends. *J. Sustain. Cem. Mater.* **2012**, *1*, 167–178. [CrossRef]
73. Rattanasak, U.; Pankhet, K.; Chindaprasirt, P. Effect of chemical admixtures on properties of high-calcium fly ash geopolymer. *Int. J. Miner. Met. Mater.* **2011**, *18*, 364–369. [CrossRef]
74. Nath, S.; Kumar, S. Influence of iron making slags on strength and microstructure of fly ash geopolymer. *Constr. Build. Mater.* **2013**, *38*, 924–930. [CrossRef]
75. Ding, Y.-C.; Cheng, T.-W.; Dai, Y.-S. Application of geopolymer paste for concrete repair. *Struct. Concr.* **2017**, *18*, 561–570. [CrossRef]
76. Zhang, M.; Zhao, M.; Zhang, G.; Mann, D.; Lumsden, K.; Tao, M. Durability of red mud-fly ash based geopolymer and leaching behavior of heavy metals in sulfuric acid solutions and deionised water. *Constr. Build. Mater.* **2016**, *124*, 373–382. [CrossRef]
77. Kusbiantoro, A.; Nuruddin, M.F.; Shafiq, N.; Qazi, S.A. The effect of microwave incinerated rice husk ash on the compressive and bond strength of fly ash based geopolymer concrete. *Constr. Build. Mater.* **2012**, *36*, 695–703. [CrossRef]
78. Torres-Carrasco, M.; Puertas, F. Waste glass in the geopolymer preparation. Mechanical and microstructural characterisation. *J. Clean. Prod.* **2015**, *90*, 397–408. [CrossRef]
79. Rashad, A.M. Properties of alkali activated fly ash concrete blended with slag. *Iran. J. Mater. Sci. Eng.* **2013**, *10*, 57–64.
80. Abhilash, P.; Sashidhar, C.; Reddy, I.R. Strength properties of Fly ash and GGBS based Geo-polymer Concrete. *Int. J. ChemTech Res.* **2016**, *9*, 350–356.
81. Oderji, S.Y.; Chen, B.; Ahmad, M.R.; Shah, S.F.A. Fresh and hardened properties of one-part fly ash-based geopolymer binders cured at room temperature: Effect of slag and alkali activators. *J. Clean. Prod.* **2019**, *225*, 1–10. [CrossRef]

82. Sarvanan, S.; Elavenil, S. Strength properties of geopolymer concrete using M-sand by assessing their mechanical characteristics. *ARPN J. Eng. Appl. Sci.* **2018**, *13*, 4028–4041.
83. Partha, S.D.; Pradib, N.; Prabir, K.S. Strength and Permeation Properties of Slag Blended Fly Ash Based Geopolymer Concrete. *Adv. Mater. Res.* **2013**, *651*, 168–173. [CrossRef]
84. Lee, B.; Kim, G.; Kim, R.; Cho, B.; Lee, S.; Chon, C.M. Strength Development Properties of Geopolymer Paste and Mortar with Respect to Amorphous Si/Al Ratio of Fly Ash. *Constr. Build. Mater.* **2017**, *151*, 512–519. [CrossRef]
85. Zhuang, X.Y.; Chen, L.; Komarneni, S.; Zhou, C.H.; Tong, D.S.; Yang, H.M.; Yu, W.H.; Wang, H. Fly Ash-Based Geopolymer: Clean Production, Properties and Applications. *J. Clean. Prod.* **2016**, *125*, 253–267. [CrossRef]
86. Wong, L.S. Durability performance of geopolymer concrete: A review. *Polymers* **2022**, *14*, 868. [CrossRef]
87. Alomayri, T. The microstructural and mechanical properties of geopolymer composites containing glass microfibres. *Ceram. Int.* **2017**, *43*, 4576–4582. [CrossRef]
88. Pongsak, J.; Horpibulsuk, S. Physical and microstructure properties of geopolymer nanocomposite reinforced with carbon nanotubes. *Mater. Today Proc.* **2019**, *17*, 1682–1692.
89. Qaidi, S.; Najm, H.M.; Abed, S.M.; Ahmed, H.U.; Al Dughaishi, H.; Al Lawati, J.; Sabri, M.M.; Alkhatib, F.; Milad, A. Fly Ash-Based Geopolymer Composites: A Review of the Compressive Strength and Microstructure Analysis. *Materials* **2022**, *15*, 7098. [CrossRef]
90. Han, Q.; Zhang, P.; Wu, J.; Jing, Y.; Zhang, D.; Zhang, T. Comprehensive review of the properties of fly ash-based geopolymer with additive of nano-SiO_2. *Nanotechnol. Rev.* **2022**, *11*, 1478–1498. [CrossRef]
91. Arafa, S.; Milad, A.; Yusoff, N.I.M.; Al-Ansari, N.; Yaseen, Z.M. Investigation into the permeability and strength of pervious geopolymer concrete containing coated biomass aggregate material. *J. Mater. Res. Technol.* **2021**, *15*, 2075–2087. [CrossRef]
92. Milad, A.; Ali, A.S.B.; Babalghaith, A.M.; Memon, Z.A.; Mashaan, N.S.; Arafa, S.; Md Yusoff, N.I. Utilisation of waste-based geopolymer in asphalt pavement modification and construction—A review. *Sustainability* **2021**, *13*, 3330. [CrossRef]
93. Toniolo, N.; Rincón, A.; Roether, J.A.; Ercole, P.; Bernardo, E.; Boccaccini, A.R. Extensive reuse of soda-lime waste glass in fly ash-based geopolymers. *Constr. Build. Mater.* **2018**, *188*, 1077–1084. [CrossRef]
94. Rosas-Casarez, C.A.; Arredondo-Rea, S.P.; Gómez-Soberón, J.M.; Alamaral-Sánchez, J.L.; Corral-Higuera, R.; Chinchillas-Chinchillas MD, J.; Acuña-Agüero, O.H. Experimental study of XRD, FTIR and TGA techniques in geopolymeric materials. *Int. J. Adv. Comput. Sci. Appl* **2014**, *4*, 221–226.
95. Al Bakri, A.M.; Kamarudin, H.; Bnhussain, M.; Nizar, I.K.; Rafiza, A.R.; Zarina, Y. The processing, characterisation, and properties of fly ash based geopolymer concrete. *Rev. Adv. Mater. Sci.* **2012**, *30*, 90–97.
96. Xiao, S.; Cai, Y.; Guo, Y.; Lin, J.; Liu, G.; Lan, X.; Song, Y. Experimental Study on Axial Compressive Performance of Polyvinyl Alcohol Fibers Reinforced Fly Ash—Slag Geopolymer Composites. *Polymers* **2021**, *14*, 142. [CrossRef]
97. Korniejenko, K.; Kejzlar, P.; Louda, P. The Influence of the Material Structure on the Mechanical Properties of Geopolymer Composites Reinforced with Short Fibers Obtained with Additive Technologies. *Int. J. Mol. Sci.* **2022**, *23*, 2023. [CrossRef]
98. Chen, X.; Zhou, M.; Shen, W.; Zhu, G.; Ge, X. Mechanical properties and microstructure of metakaolin-based geopolymer compound-modified by polyacrylic emulsion and polypropylene fibers. *Constr. Build. Mater.* **2018**, *190*, 680–690. [CrossRef]
99. Hemalatha, T.; Ramaswamy, A. A review on fly ash characteristics—Towards promoting high volume utilization in developing sustainable concrete. *J. Clean. Prod.* **2017**, *147*, 546–559. [CrossRef]
100. Le, T.A.; Le, S.H.; Nguyen, T.N.; Nguyen, K.T. Assessment of the Rheological and Mechanical Properties of Geopolymer Concrete Comprising Fly Ash and Fluid Catalytic Cracking Residue as Aluminosilicate Precursor. *Appl. Sci.* **2021**, *11*, 3032. [CrossRef]
101. Salih, M.A.; Ali AA, A.; Farzadnia, N. Characterization of mechanical and microstructural properties of palm oil fuel ash geopolymer cement paste. *Constr. Build. Mater.* **2014**, *65*, 592–603. [CrossRef]
102. Rajini, B.; Rao, A.N.; Sashidhar, C. Micro-level studies of fly ash and GGBS–based geopolymer concrete using Fourier transform infra-red. *Mater. Today Proc.* **2021**, *46*, 586–589. [CrossRef]
103. Frydrych, M.; Hýsek, Š.; Fridrichová, L.; Le Van, S.; Herclík, M.; Pechočiaková, M.; Le Chi, H.; Louda, P. Impact of Flax and Basalt Fibre Reinforcement on Selected Properties of Geopolymer Composites. *Sustainability* **2019**, *12*, 118. [CrossRef]
104. Zhao, J.; Wang, K.; Wang, S.; Wang, Z.; Yang, Z.; Shumuye, E.D.; Gong, X. Effect of elevated temperature on mechanical properties of high-volume fly ash-based geopolymer concrete, mortar and paste cured at room temperature. *Polymers* **2021**, *13*, 1473. [CrossRef]
105. Tayeh, B.A.; Zeyad, A.M.; Agwa, I.S.; Amin, M. Effect of elevated temperatures on mechanical properties of lightweight geopolymer concrete. *Case Stud. Constr. Mater.* **2021**, *15*, e00673. [CrossRef]
106. Vogt, O.; Ukrainczyk, N.; Ballschmiede, C.; Koenders, E. Reactivity and microstructure of metakaolin based geopolymers: Effect of fly Ash and liquid/solid contents. *Materials* **2019**, *12*, 3485. [CrossRef]
107. Jamil, N.H.; Abdullah, M.M.A.B.; Pa, F.C.; Mohamad, H.; Ibrahim, W.M.A.W.; Amonpattaratkit, P.; Gondro, J.; Sochacki, W.; Ibrahim, N. Self-fluxing mechanism in geopolymerization for low-sintering temperature of ceramic. *Materials* **2021**, *14*, 1325. [CrossRef]
108. Haruna, S.; Mohammed, B.S.; Wahab, M.M.A.; Kankia, M.U.; Amran, M.; Gora, A.U.M. Long-Term Strength Development of Fly Ash-Based One-Part Alkali-Activated Binders. *Materials* **2021**, *14*, 4160. [CrossRef]
109. Zhang, H.; Li, L.; Long, T.; Sarker, P.K.; Shi, X.; Cai, G.; Wang, Q. The effect of ordinary portland cement substitution on the thermal stability of geopolymer concrete. *Materials* **2019**, *12*, 2501. [CrossRef]

110. Burduhos Nergis, D.D.; Vizureanu, P.; Sandu, A.V.; Burduhos Nergis, D.P.; Bejinariu, C. XRD and TG-DTA Study of New Phosphate-Based Geopolymers with Coal Ash or Metakaolin as Aluminosilicate Source and Mine Tailings Addition. *Materials* **2021**, *15*, 202. [CrossRef] [PubMed]
111. Irshidat, M.R.; Al-Nuaimi, N.; Rabie, M. Sustainable utilisation of waste carbon black in alkali-activated mortar production. *Case Stud. Constr. Mater.* **2021**, *15*, e00743.
112. Khan, M.; Cao, M.; Ai, H.; Hussain, A. Basalt fibers in modified whisker reinforced cementitious composites. *Period. Polytech. Civ. Eng.* **2022**, *66*, 344–354. [CrossRef]
113. Xie, C.; Cao, M.; Guan, J.; Liu, Z.; Khan, M. Improvement of boundary effect model in multi-scale hybrid fibers reinforced cementitious composite and prediction of its structural failure behavior. *Compos. Part B Eng.* **2021**, *224*, 109219. [CrossRef]
114. Khan, M.; Cao, M.; Xie, C.; Ali, M. Effectiveness of hybrid steel-basalt fiber reinforced concrete under compression. *Case Stud. Constr. Mater.* **2022**, *16*, e00941. [CrossRef]
115. Cao, M.; Khan, M. Effectiveness of multiscale hybrid fiber reinforced cementitious composites under single degree of freedom hydraulic shaking table. *Struct. Concr.* **2021**, *22*, 535–549. [CrossRef]
116. Cao, M.; Khan, M.; Ahmed, S. Effectiveness of Calcium Carbonate Whisker in Cementitious Composites. *Period. Polytechnica. Civ. Eng.* **2022**, *64*, 265. [CrossRef]
117. Zhang, N.; Yan, C.; Li, L.; Khan, M. Assessment of fiber factor for the fracture toughness of polyethylene fiber reinforced geopolymer. *Constr. Build. Mater.* **2022**, *319*, 126130. [CrossRef]
118. Öz, H.Ö.; Doğan-Sağlamtimur, N.; Bilgil, A.; Tamer, A.; Günaydin, K. Process Development of Fly Ash-Based Geopolymer Mortars in View of the Mechanical Characteristics. *Materials* **2021**, *14*, 2935. [CrossRef]
119. Kljajević, L.; Nenadović, M.; Ivanović, M.; Bučevac, D.; Mirković, M.; Mladenović Nikolić, N.; Nenadović, S. Heat Treatment of Geopolymer Samples Obtained by Varying Concentration of Sodium Hydroxide as Constituent of Alkali Activator. *Gels* **2022**, *8*, 333. [CrossRef]
120. Najm, H.M.; Ahmad, S.; Khan, R.A. Mechanical and Microstructural Analysis of Waste Ceramic Optimal Concrete Reinforced by Hybrid Fibers Materials: A Comprehensive Study. *J. Archit. Environ. Struct. Eng. Res.* **2022**, *5*, 11–33. [CrossRef]
121. Najm, H.M.; Nanayakkara, O.; Ahmad, M.; Sabri Sabri, M.M. Mechanical Properties, Crack Width, and Propagation of Waste Ceramic Concrete Subjected to Elevated Temperatures: A Comprehensive Study. *Materials* **2022**, *15*, 2371. [CrossRef]
122. Najm, H.M.; Nanayakkara, O.; Ahmad, M.; Sabri Sabri, M.M. Colour Change of Sustainable Concrete Containing Waste Ceramic and Hybrid Fibre: Effect of Temperature. *Materials* **2022**, *15*, 2174. [CrossRef]
123. Çelik, A.İ.; Özkılıç, Y.O.; Zeybek, Ö.; Özdöner, N.; Tayeh, B.A. Performance Assessment of Fiber-Reinforced Concrete Produced with Waste Lathe Fibers. *Sustainability* **2022**, *14*, 11817. [CrossRef]
124. Najm, H.M.; Ahmad, S. Effect of Elevated Temperatures Exposure on the Mechanical Properties of Waste Ceramic Concrete Reinforced with Hybrid Fibers Materials. *Sigma J. Eng. Nat. Sci.* 2021, *in press*.
125. Aksoylu, C.; Özkılıç, Y.O.; Hadzima-Nyarko, M.; Işık, E.; Arslan, M.H. Investigation improvement in shear performance of reinforced concrete beams produced with recycled steel wires from waste tyre. *Sustainability* **2022**, *14*, 13360. [CrossRef]
126. Najm, H.M.; Ahmad, S. The Use of Waste Ceramic Optimal Concrete for A Cleaner and Sustainable Environment—A Case Study of Mechanical Properties. *Civ. Environ. Eng. Rep.* **2022**, *32*, 85–102. [CrossRef]
127. Karalar, M.; Özkılıç, Y.O.; Deifalla, A.; Aksoylu, C.; Arslan, M.H.; Ahmad, M.; Sabri, M.M.S. Improvement in Bending Performance of Reinforced Concrete Beams Produced with Waste Lathe Scraps. *Sustainability* **2022**, *14*, 12660. [CrossRef]
128. Najm, H.M.; Ahmad, S.; Submitter, Y. Artificial Neural Networks for Evaluation & Prediction of the Mechanical Properties of Waste Ceramic Optimal Concrete Exposed to Elevated Temperature. *Available SSRN* **2021**, 4032028. [CrossRef]
129. Hussein, O.H.; Ibrahim, A.M.; Abd, S.M.; Najm, H.M.; Shamim, S.; Sabri, M.M.S. Hybrid Effect of Steel Bars and PAN Textile Reinforcement on Ductility of One-Way Slab Subjected to Bending. *Molecules* **2022**, *27*, 5208. [CrossRef]
130. Najm, H.M.; Ahmad, S. The effect of metallic and non-metallic fiber on the mechanical properties of waste ceramic concrete. *Innov. Infrastruct. Solut.* **2021**, *6*, 204. [CrossRef]
131. Qaidi, S.; Najm, H.M.; Abed, S.M.; Özkılıç, Y.O.; Al Dughaishi, H.; Alosta, M.; Sabri, M.M.S.; Alkhatib, F.; Milad, A. Concrete Containing Waste Glass as an Environmentally Friendly Aggregate: A Review on Fresh and Mechanical Characteristics. *Materials* **2022**, *15*, 6222. [CrossRef] [PubMed]
132. Nanayakkara, O.; Najm, H.M.; Sabri, M.M.S. Effect of Using Steel Bar Reinforcement on Concrete Quality by Ultrasonic Pulse Velocity Measurements. *Materials* **2022**, *15*, 4565. [CrossRef] [PubMed]